Studies on Nematic Liquid Crystal Composite Langmuir Blodgett Films: Effects of SiO_2 Nano-Particles

A Dissertation

Submitted

in partial fulfillment of the requirement for

the award of the degree of

MASTER OF SCIENCE (M.Sc.)

IN

PHYSICS

By

Harveen Kaur

(Roll no: 301004021)

Under the supervision of

Dr. K.K. Raina

School of Physics and Materials Science

Thapar University

Patiala (Punjab)-147004, India

July 2012

CERTIFICATE

This is to certify that the thesis entitled "**Studies on Nematic Liquid Crystal Composite Langmuir Blodgett Films: Effects of SiO_2 Nano-Particles**" submitted by **Harveen Kaur**, Roll No. **301004021** in the partial fulfillment of the requirement for the award of the degree of M.Sc. from School of Physics and Material Science, Thapar University, Patiala, is a record of candidate's own work carried by her under my supervision and guidance. The experimental part embodied in this report has not been submitted in part or full to any other university or institute for the award of any degree.

Dr. K.K. Raina

Deputy Director and Distinguished Professor

Thapar University, Patiala-147004

Punjab, India

Countersigned By:

Dr. Kulvir Singh

Associate Professor and Head

School of Physics and Material Science

Thapar University

Patiala

Dr. S.K. Mohapatra

Dean of Academic Affairs

Thapar University

Patiala

ACKNOWLEDGEMENT

Several peoples have collaborated in the developed and accomplishment of my thesis work.

I would like to express my sincere gratitude to my esteemed and worthy supervisor **Dr. K.K. Raina, Deputy Director and Distinguished Professor, School of Physics and Material Science, Thapar University** for his insight help, guidance, effective supervision and encouragement in carry out this dream comes true. His wide knowledge and his logical way of thinking have been of great value for me.

I am deeply grateful to **Dr. Kulvir Singh, Associate Professor and Head, School of Physics and Material Science** for his detailed and constructive comments and for his important support throughout the work.

I wish to express my sincere thanks to **Dr. Manoj Sharma, P.G. incharge, School of Material and Physics Science** for his support and encouragement.

I am deeply indebted to my teachers, School of Material and Physics Science, Thapar University, Patiala (Punjab). Their ideas and concepts made a remarkable influence on my understanding in the field of Physics.

I wish my heartfelt thanks to research scholars **Mrs. Ramneek Kaur, Ms. Gurpreet Kaur, Mr. Ravi Shukla, Mr. Rishi Kumar and Dr. Dinesh Pathak** for their generous works and good wishes.

I have no words to express to **my parents** who always a constant inspiration for me and supporting me spiritually throughout my life.

Parveen Kaur

Parveen Kaur

Roll no. 800004021

Date: 5 July 2012.

Dedicated

to

My Parents

ABSTRACT

Langmuir Blodgett monolayers of eutectic nematic liquid crystal and its mixture with polyvinyl alcohol (PVA) capped SiO_2 nanoparticles were deposited on quartz substrate in Y-type mode. PVA capped SiO_2 nanoparticles were characterized by Fourier Transformation Infrared Spectroscopy (FTIR). Surface pressure-area isotherm profiles were studied for each monolayer, as various phase changes were observed during constant compression of barriers. The Langmuir monolayer of nematic liquid crystal mixture showed hysteresis during multiple isotherms because of the mixed amphiphilic nature of nematic liquid crystal molecules while PVA capped SiO_2 nanoparticles showed no hysteresis during isotherm cycles due to elastic nature of the polymer. Elasticity profile of monolayer has been studied as a function of mean molecular area (MMA). Normalized area profiles decrease constantly with time ensuring about constant film compression. Equilibrium stabilized surface pressure (ESP) was attained during each deposition. Topography of monolayer has been investigated through Atomic Force Microscope (AFM).

List of Content

List of Tables

List of Figure

CHAPTER – 1

1.1 Introduction

A thin film is layer of a material ranging from fraction of a nanometer to several micrometers. The properties of thin films differ from the bulk material because of small thickness, unique physical structure which is direct consequence of the growth process and large surface to volume ratio.

A very old method of forming thin films is the beating of gold to form gold leaf. Too much stress applied on the gold leads to rupture, thus imposing limitations on the thickness of film obtained in this way. But the sample so obtained cannot be treated as thin film because of structural arrangement of atoms. The thin film may also be formed form liquid or paste. But such films mainly belong to category of thick films. The floating of one liquid on another immiscible liquid in a very small quantity leads to the formation of thin films. This phenomenon is used in Langmuir Blodgett deposition. Langmuir Blodgett is a novel process and is very suitable for deposition of soft materials.

1.2 History of Langmuir Blodgett Film

In 1774, Benjamin Franklin discovered thin film on air water interface [1]. In the late 19th century Agnes Pockles, a German pioneer in chemistry, discovered the influence of impurities on the surface tension of water by using a rudimentary surface balance in her kitchen sink. This system was a precursor to the Langmuir trough [2].

In the early 20th century Irving Langmuir, an American chemist and physicist, was the first to perform systematic studies on floating monolayers on water. He was the first to give the modern understanding of monolayer structure at the molecular level, in particular the fact that the molecules show a preferential orientation. The systems to study floating monolayers on water are now named after him: Langmuir films.

In 1932 he was awarded the Nobel Prize for his work on surface chemistry. Katherine Blodgett showed that it was possible to go further and to deposit many monolayers onto the same substrate, thus building up multilayer film of any required thickness. Deposited monolayers of any thickness are now known as Langmuir Blodgett (LB) films [3].

1.3 Langmuir Blodgett Film

Langmuir Blodgett film contains monolayer or multilayers of an organic material, deposited from air-liquid interface to a solid by immersing or emersion the solid substrate into the liquid. A monolayer is adsorbed homogeneously with each immersion or emersion step, thus films with very accurate thickness can be formed. By knowing thickness of monolayer, we can calculate thickness of multilayer. As Langmuir Blodgett is uniform deposition process. For amphiphilic character is must for deposition shown Fig. 1.1. The hydrophilic part of an amphiphilic molecule (usually called the head) is a polar molecule whereas the hydrophobic part (called the tail) is a hydrocarbon chain 8-16 Carbon atom in length [4, 5].

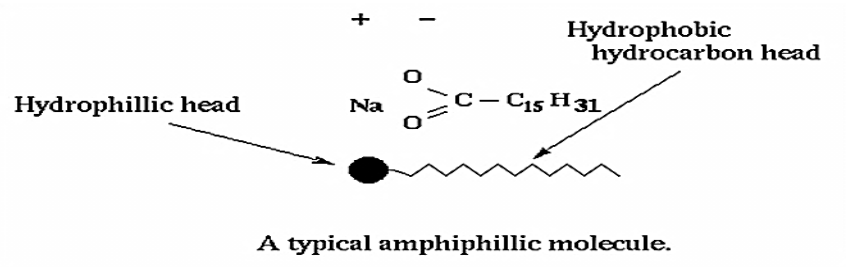

Fig. 1.1 A Sodium Salt Palmatic acids with COO- group are hydrophilic and C_{15} long carbon chain is hydrophobic.

1.4 PHYSICAL INSIGHT

LB films are formed when amphiphilic molecules interact with air at an air-water interface. Amphphiilic molecules have hydrophobic 'tails' and hydrophilic 'heads'. The heads are hydrophilic, they are attracted toward water surface. The tails are hydrophobic, their exposure to air is favoured over that to water. The overall effect is reduction in the surface energy (or equivalently, surface tension of water).

For very small concentrations, far less than critical micelle concentration (CMC), the amphiphilic molecules execute a random motion on the water-air interface. This motion can be thought to be similar to the motion of ideal gas molecules enclosed in a container. The corresponding thermodynamic variables for the surfactant system are surface pressure (Π), surface area (A) and number of surfactant molecules (N). This system behaves similarly to a gas in a container. The density of surfactant molecules as well as the surface pressure increase upon reducing the surface area A (compression of the gas). Further compression of the surfactant molecules on the surface shows behavior similar to phase transitions. The gas gets compressed into liquid and ultimately into a perfectly closed packed array of the surfactant molecules on the

surface corresponding to a solid state. Instruments like the Langmuir–Blodgett trough can be used to quantify such phenomena.

1.5 Surface Pressure-Area Isotherm

Surface pressure-area isotherm can be defined as a measurement of surface pressure as changing the available area for each molecule in a floating monolayer (Langmuir film) at room temperature. This two-dimensional analogue of a pressure is called surface pressure $\prod$ and is given by the relationship

$$\prod = \gamma - \gamma_{\circ}$$

where γ is the surface tension in absence of a monolayer and $\gamma_{\circ}$ the surface tensions with the monolayer present [6].

The most important indicator of the monolayer properties of an amphiphilic material (usually used to create Langmuir films) is given by measuring the surface pressure as a function of the area of water surface available to each molecule. Usually an isotherm is recorded at room temperature by compressing the film (reducing the area with the barriers) at a constant rate while continuously monitoring the surface pressure. Depending on the material being studied, repeated compressions and expansions may be necessary to achieve a reproducible trace.

When the monolayer is compressed it can pass through several different phases which are identified as discontinuities in the isotherm. The phase behavior of the monolayer is mainly determined by the physical and chemical properties of the amphiphilic material, the sub-phase temperature and the sub-phase composition [7].

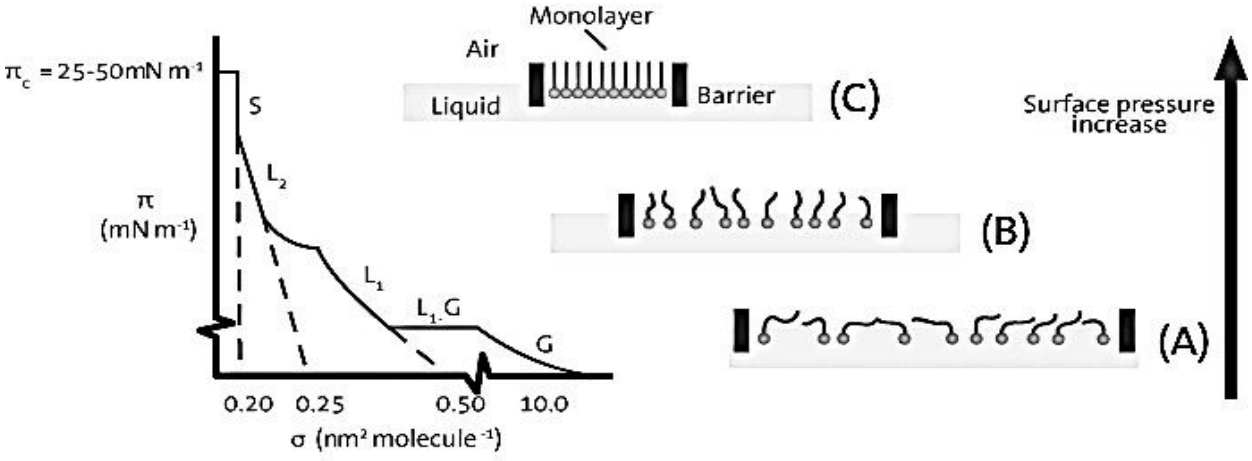

Fig. 1.2 Surface pressure – Area isotherm

In beginning when barriers are for away monolayers exist in the gaseous state (G) and can on compression undergoes a phase transition to the liquid-expanded state (L_1). After passing through on intermediate state (L_1G), L_1G is liquid gas combined phase. Upon further compression, the L_1 phase undergoes a transition to the liquid-condensed state (L_2) and at further compression the monolayer finally reaches the solid state (S). If the monolayer is further compressed after reaching the S state the monolayer will collapse into three-dimensional structures. The collapse is generally seen as a rapid decrease in the surface pressure or as a horizontal break in the isotherm if the monolayer is in a liquid state.

1.6 Method for Langmuir Blodgett Film Deposition

Monolayer deposition on the substrate by two methods:

1. Horizontal deposition: Horizontal deposition is formed by one or several Langmuir films deposited onto a solid surface by horizontal dipping of the solid substrate through air-water interface. The films obtained can be highly organized ranging from ultrathin monolayer to multilayer structures built up of hundreds of monolayers. The film is form by horizontal dipping of solid substrate know as Langmuir Schaefer Technique.

2. Vertical deposition: Vertical deposition is formed by one or several films deposited onto a solid surface by vertical dipping of the solid substrate from the gas phase into the liquid phase or liquid phase into gas phase. The film is formed by vertical dipping of solid substrate know as Langmuir Blodgett Technique.

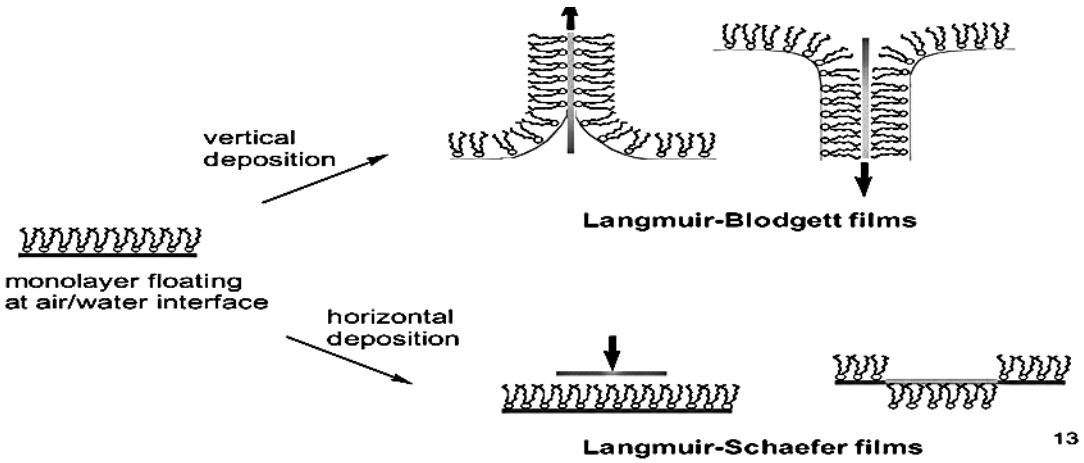

Fig 1.3 Vertical deposition and Horizontal deposition

Repeated deposition can be performed to obtain well organized multilayers on the solid substrate. There are several parameters that effect on what type of LB film is produced. These are the nature of the spread film decided whether we add a hydrophilic or hydrophobic substrate, the sub-phase composition and temperature are necessary for alignment of film, the surface pressure during the deposition and the deposition speed should be constant for good deposition and type and nature of the solid substrate.

Different kind of LB multilayers can be produced and obtained by successive deposition of monolayers on the same substrate. LB multilayer can be formed in different ways. The most common one is the Y-type multilayer which is produced when the monolayer deposits to the solid substrate in both up and down directions. When the monolayer deposits only in the up or down direction the multilayer structure is called either Z-type or X-type respectively. Intermediate structures are sometimes observed for some LB multilayers and they are often referred to be XY-type multilayers.

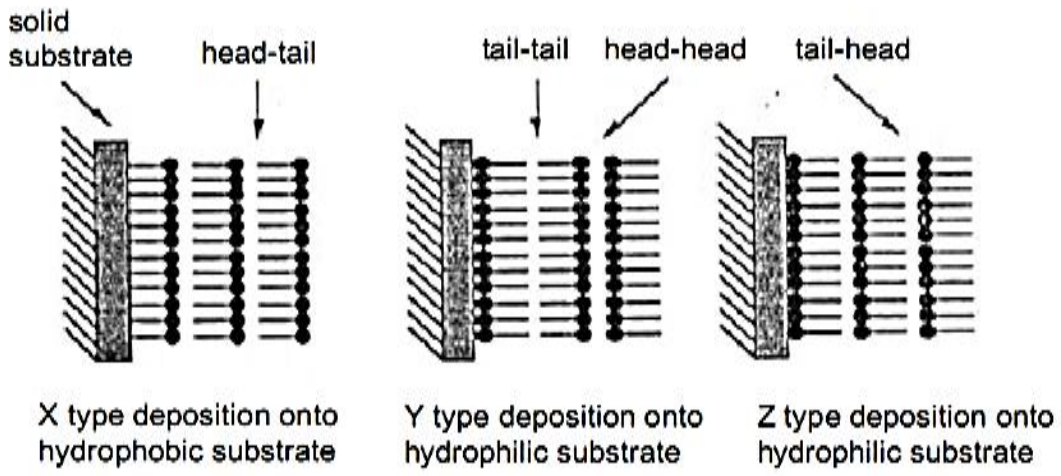

Fig. 1.4 Different type of LB film deposition

1.7 Material Used For LB Deposition

Many amphiphilic materials including liquid crystal have been deposited by using Langmuir Blodgett technique. Fatty Acids and related compounds which have consist a simple long chain fatty acid consists of an alkyl chain and terminating in a carboxylic acid group (COOH). The polar acid head confers water solubility while the hydrocarbon chain prevents it. It is the balance between these two opposing forces that results in the formation of the insoluble monolayer at the air/water interface. Conductive polymers or more precisely intrinsically

conducting polymers (ICPs) or organic polymers that conduct electricity are used in LB deposition. Amphiphilic derivatives of aromatic compounds in which two or more benzene rings are fused or superimposed together at ortho positions may also be built up into multilayer films e.g. are anthracene (three rings) and pyrene (four rings). Long chain fatty acid materials all possess relatively low melting point and poor mechanical properties. Polymeric materials on the other hand, are much more robust [8].

1.8 Comparison of LB with other Deposition Techniques

Techniques fall into two broad categories:-

1. Chemical Deposition Technique
2. Physical Deposition Technique

1.8.1 Chemical Deposition Technique

A fluid precursor undergoes a chemical change at a solid surface, leaving a solid layer. An everyday example is the formation of soot on a cool object when it is placed inside a flame. Since the fluid surrounds the solid object, deposition happens on every surface with little regard to direction, thin films from chemical deposition techniques tend to be conformal rather than directional [9-11].

• Chemical solution deposition (CSD) uses a liquid precursor, usually a solution of organometallic powders dissolved in an organic solvent. This is a relatively inexpensive, simple thin film process that is able to produce stoichiometrically accurate crystalline phases.

• Chemical vapor deposition (CVD) generally uses a gas-phase precursor, often a halide or hydride of the element to be deposited. In the case of Metal Organic Chemical vapor deposition (MOCVD), an organometallic gas is used. Commercial techniques often use very low pressures of precursor gas.

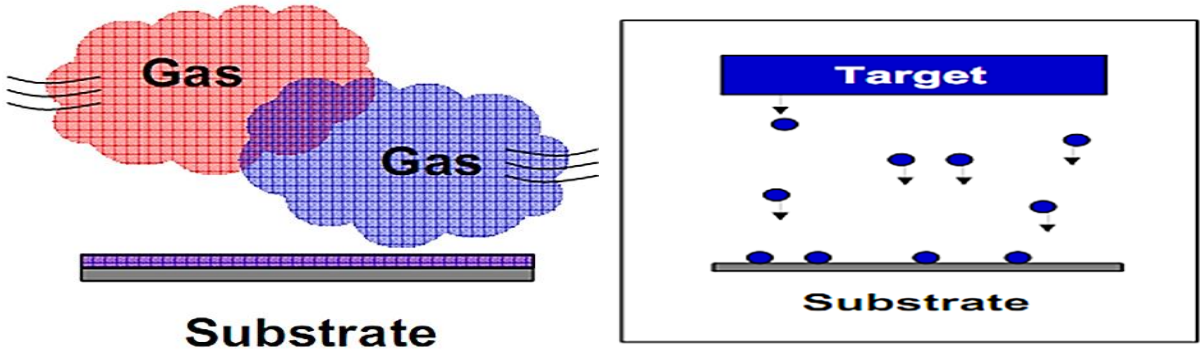

Fig.1.5 (a) Chemical Vapour Deposition and (b)Physical Vapour Deposition

1.8.2 Physical Deposition Technique

Physical deposition uses mechanical or thermodynamic means to produce a thin film of solid. Most engineering materials are held together by relatively high energies and chemical reactions are not used to store these energies, commercial physical deposition systems tend to require a low pressure vapor environment to function properly can be classified as physical vapor deposition (PVD). PVD is a process by which a thin film of material is deposited on a substrate according to the following sequence of steps:

1) The material to be deposited is converted into vapor by physical means.

2) The vapor is transported across a region of low pressure from its source to the substrate.

3) The vapor undergoes condensation on the substrate to form the thin film. In Very Large Scale Integration fabrication, the most widely-used method of accomplishing PVD of thin films is by sputtering.

Different Type of PVD:-

1. Thermal Evaporator
2. Sputtering
3. Pulsed Laser Deposition

1. Thermal Evaporator

A thermal evaporator uses an electric resistance heater to melt the material and raise its vapor pressure to a useful range. This is done in a high vacuum, both to allow the vapor to reach the substrate without reacting with or scattering against other gas-phase atoms in the chamber and reduce the incorporation of impurities from the residual gas in the vacuum chamber. Obviously, only materials with a much higher vapor pressure than the heating element can be deposited without contamination of the film. Molecular beam epitaxy is a particular sophisticated form of thermal evaporation.

An electron beam evaporator fires a high-energy beam from an electron gun to boil a small spot of material, since the heating is not uniform, lower vapor pressure materials can be deposited. The beam is usually bent through an angle of 270° in order to ensure that the gun filament is not directly exposed to the evaporant flux. Typical deposition rates for electron beam evaporation range from 1 to 10 nanometres per second.

2. Sputtering

Sputtering relies on a plasma (usually a noble gas, such as argon) to knock material from a target a few atoms at a time. The target can be kept at a relatively low temperature, since the process is not one of evaporation, making this one of the most flexible deposition techniques. It is especially useful for compounds or mixtures, where different components would otherwise tend to evaporate at different rates. Note, sputtering's step coverage is more or less conformal.It is also widely used in the optical media. The manufacturing of all formats of CD, DVD and BD are basically done with the help of this technique. It is a fast technique and also it provides a good thickness control. Presently, Nitrogen and Oxygen gases are also being used in sputtering.

3. Pulse Laser Deposition

Pulsed laser deposition systems work by an ablation process. Pulses of focused laser light vaporize the surface of the target material and convert it to plasma, this plasma usually reverts to a gas before it reaches the substrate [12].

1.9 Advantage of LB Films

The LB technique is one of the most promising techniques for preparing highly organized thin films as it enables:

1. Precise control of the monolayer thickness and phase state.
2. Homogeneous deposition of a monolayer over large areas (several cm^2).
3. Possibility to prepare multilayer films (from 2 to hundreds of layers).
4. Structures with varying layer composition (two different surfactants) and orientation.
5. Deposition of a large variety of surfactants on different kinds of solid substrate.

1.10 Applications of LB Films

Many possible applications have been suggested over years for Langmuir Blodgett films. Their characteristics are extremely thin films and high degree of structural order. These films have different optical, electrical and biological properties which are composed of some specific organic compounds. Organic compounds usually have more positive responses than inorganic materials for outside factors (pressure, temperature or gas change).

1. LB film of liquid crystal can be used to reduce thickness from nanometer to micro meter. Thus width of LC displays can be reduced to great extant.

2. LB films can be used as passive layers in MIS (metal-insulator-semiconductor) which have more open structure than silicon oxide and they allow gases to penetrate to the interface more easily and have obvious effects.
3. LB films also can be used as biological membranes. Lipid molecules with the fatty and polar region have received extended attention because of being adequately suited to the Langmuir method. This kind of biological membranes can be investigated in the mode of drug action, the chemistry of biologically active molecules and the modeling of biological system.
4. LB is possible to propose field effect devise for observing the immunological response and enzyme-substrate reactions by collecting biological molecules such as antibodies and enzymes in insulating LB films.
5. LB can be used to make anti-reflective glass but at the same time allowing 99% of visible light to pass through.
6. Glucose biosensor can be use of poly (3-hexylthiopene) as Langmuir Blodgett film which entraps glucose-oxide and transfers it to a coated indium-tin-oxide glass plate.
7. Langmuir Blodgett films are inherently 2D structures and can be built up layer by layer by dipping hydrophobic or hydrophilic substrates into a liquid sub phase.
8. Langmuir Blodgett patterning is a new paradigm for large area patterning with meso-structured features [4, 5, 13].

1.11 References

1. Franklin B., Brownrigg W. and Farish M., Philosophical Transactions, 445, **64**, (1774).
2. Pockets A., Nature, 418, **46**, (1892).
3. Blodgett K. B., Journal of the American Chemical Society, 1007, **57**, (1935).
4. Xiaodong C., Steven L., Michael H., Nan L., Harald F. and Lifeng C., Accounts of Chemical Research, 393, **40**, (2007).
5. Oliver P., Anton F., Karin L., Rainer J. and Motomu T., Journal of the American Chemistry Society, 1258, **127,** (2005).
6. Osvaldo V. and Oliveira J., Journal of Physics, 2, **22**, (1992).
7. Yang P. and Kim F., Chem Phys Chem, 503, **3**, (2002).
8. Chovelon J.M., Provence M., Penault N.J., Alexandre S. and Valleton J.M., Material Science and Engineer, 78, **22**, (2002).

9. Schropp R.E.I., Stannowski B., Brockhoff A.M., Veenendaal P.A.T.T. and Rath J.K., Material Physics Mech., 73, **1**, (2000).
10. Costello M., Tossell D., Reece D., Brierley C. and Savage J., Diamond and Related Materials, 1137, **3**, (1994).
11. Dobkin D.M. and Zuraw M.K., ***Principles of Chemical Vapor Deposition***, Publisher: Springer (2003).
12. Bunshah and Roitan F., ***Deposition Technologies for Films and Coatings***, Publisher: Noyes (1994).
13. Corkery R.W., Langmuir, 3591, **13,** (1997).

CHAPTER – 2

2.1 Experiment Set Up of Langmuir Blodgett (LB) Film

The experimental set-up of the LB film has computer controller interface as shown in Fig. 2.1. The LB technique can be divided into two parts: the first one includes the building of the pressure till the condensed monolayer is formed and the second one includes the dipping of the substrate in the condensed monolayer phase for its deposition.

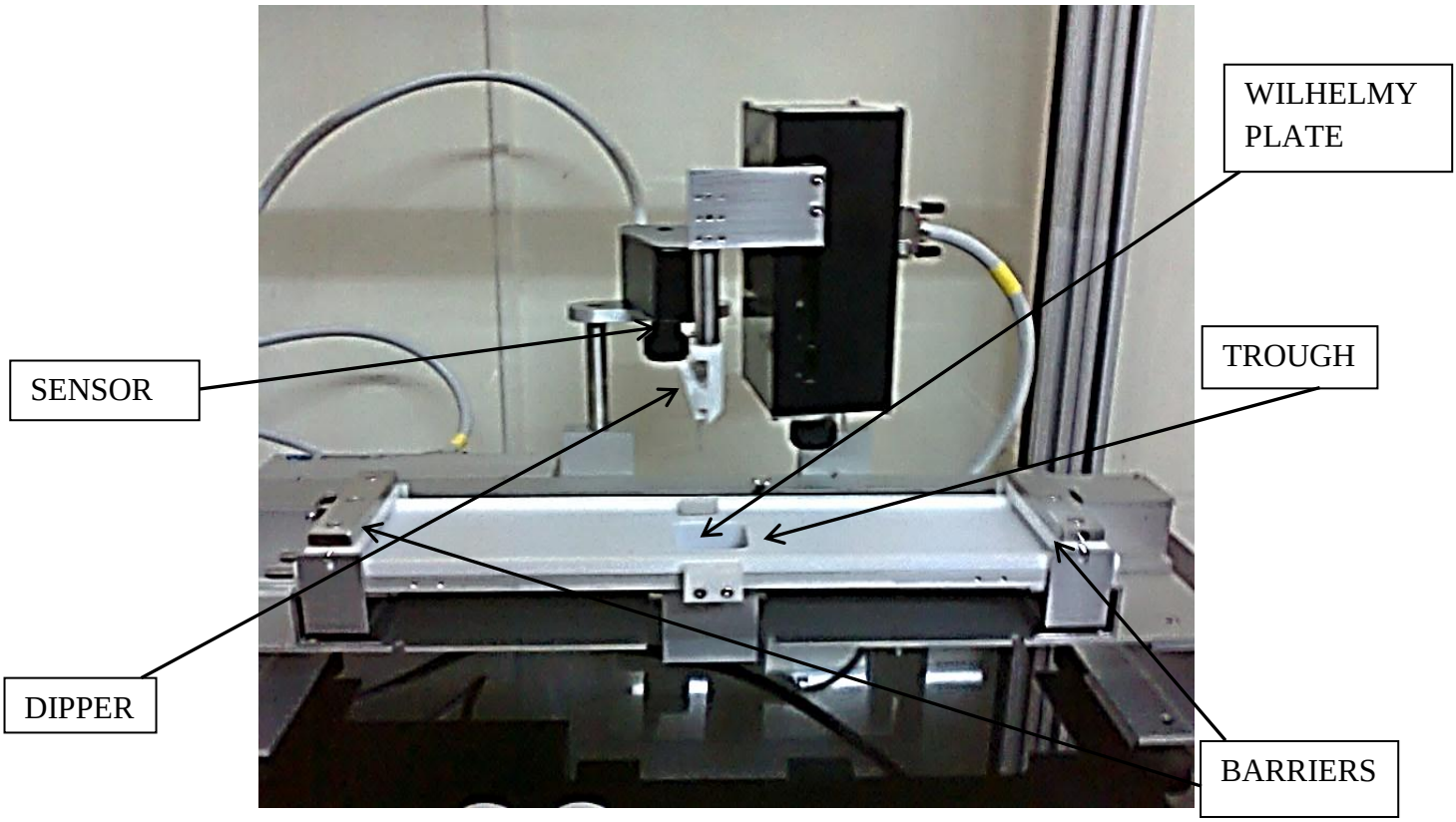

Fig. 2.1 Langmuir-Blodgett trough and set-up assembly

2.2 Parts of Experiment Set up of LB Film

2.2.1 Trough

The Langmuir Blodgett trough general objective is to create, modify and study the properties of monolayers at gas-liquid or liquid-liquid interface of amphiphilic molecules. Amphiphilic molecules are one that contains both a hydrophobic and hydrophilic domain (e.g. soaps and detergents). The LB trough helps to prepare a monolayer of amphiphilic molecules on the surface of a liquid and then compress or expand these molecules on the surface, thereby modifying the molecular density or area per molecule. This is accomplished by placing a sub-

phase (usually di ionized water) in a trough, spreading a given amphiphile over the surface and then compressing the surface with barriers.

The trough was first constructed from metals such as brass. However difficulties arose with contamination of the sub-phase by metal ions. To combat this, glass troughs were used for a time, with a wax coating to prevent contamination from glass pores. This was eventually abandoned in favor of plastics that were insoluble in ordinary solvents, such as Teflon (poly-tetrafluoro ethylene). Teflon is chemically inert, making it a highly suitable material and the most commonly used for troughs today. Occasionally metal or glass troughs coated with a thin layer of Teflon are used. It can be deposited at maximum temperature up to 60^0C with Teflon Trough [1].

2.2.2 Barriers

Different mechanisms have been used to compress or expand the monolayers throughout the development of the LB trough. In their first experiments, Langmuir and Blodgett used flexible silk threads rubbed with wax to enclose and compress the monolayer film. Most commonly used systems are made of movable Teflon barrier blocks that slide parallel to the walls of the trough and are in contact with the top of the fluid. Another version with a variable perimeter working zone is the circular trough in which the monolayer is located between two radial barriers. A constant perimeter trough was developed later in which the barrier is a flexible Teflon tape wrapped around three pairs of rollers. One of the pairs is fixed and the other two are movable on trolleys, so that the length of the tape remains constant as the area of the working zone is changed. Some troughs allow for preparation and deposition of alternating monolayers by having two separate working zones that can be compressed independently or synchronously by the barriers. We use Derlin barriers in our experiment.

2.2.3 Substrate

It is a substance that on which transfer of condensed monolayer transfer takes place. The substrate can be of two types: hydrophilic (e.g. glass etc.) or hydrophobic (e.g. mica etc.). Now there are many parameters associated with the substrate surface that can influence the deposition:
1. Its exact chemical composition may affect ion exchange in the substrate surface (whether it contains gaps or voids) is also important in determining the quality of the deposited layer.

2. The adhesion of the first layer to the underlying substrate is particularly critical and will determine the quality of the subsequent layers.

2.2.4 Surface Balance

The surface pressure is measured by using the Wilhelmy plate method (round rod optional). The Wilhelmy plate is a carefully sandblasted platinum plate or a clean paper plate, which is put partly under the surface of the sub-phase. Normal practice is to position the plate so that one third of it is under the sub-phase. The force acting on the plate depends on surface pressure. This force is measured using the electro balance [1].

2.3 Characterization Techniques

We are going to characterize the LB film by many techniques e.g. Atomic Force Microscope (AFM), Fourier Transformation IR Spectroscopy (FTIR) and many more. The characterization technique provides the information about the texture, thickness, various bonds involved etc.

2.3.1 Fourier Transformation IR Spectroscopy (FTIR)

Infrared (IR) spectroscopy is a useful technique for characterizing materials and providing information on the molecular structure, dynamics and environment of a compound. When irradiated with infrared light (photons), a sample can transmit, scatter or absorb the incident radiation. Absorbed infrared radiation usually excites molecules into higher energy vibrational states. This can occur when the energy (frequency) of the light matches the energy difference between two vibrational states (or the frequency of the corresponding molecular vibration).

Infrared spectroscopy is particularly useful for determining functional groups present in a molecule. Many functional groups vibrate at nearly the same frequencies independent of their molecular environment. This makes infrared spectroscopy useful in materials characterization. Further, many subtle structural details can be gleaned from frequency shifts and intensity changes arising from the coupling of vibrations of different chemical bonds and functional groups [2-4].

The following information can be obtained by FTIR:-

1. It can identify unknown materials.
2. It can determine the quality or consistency of a sample.
3. It can determine the amount of components in a mixture.

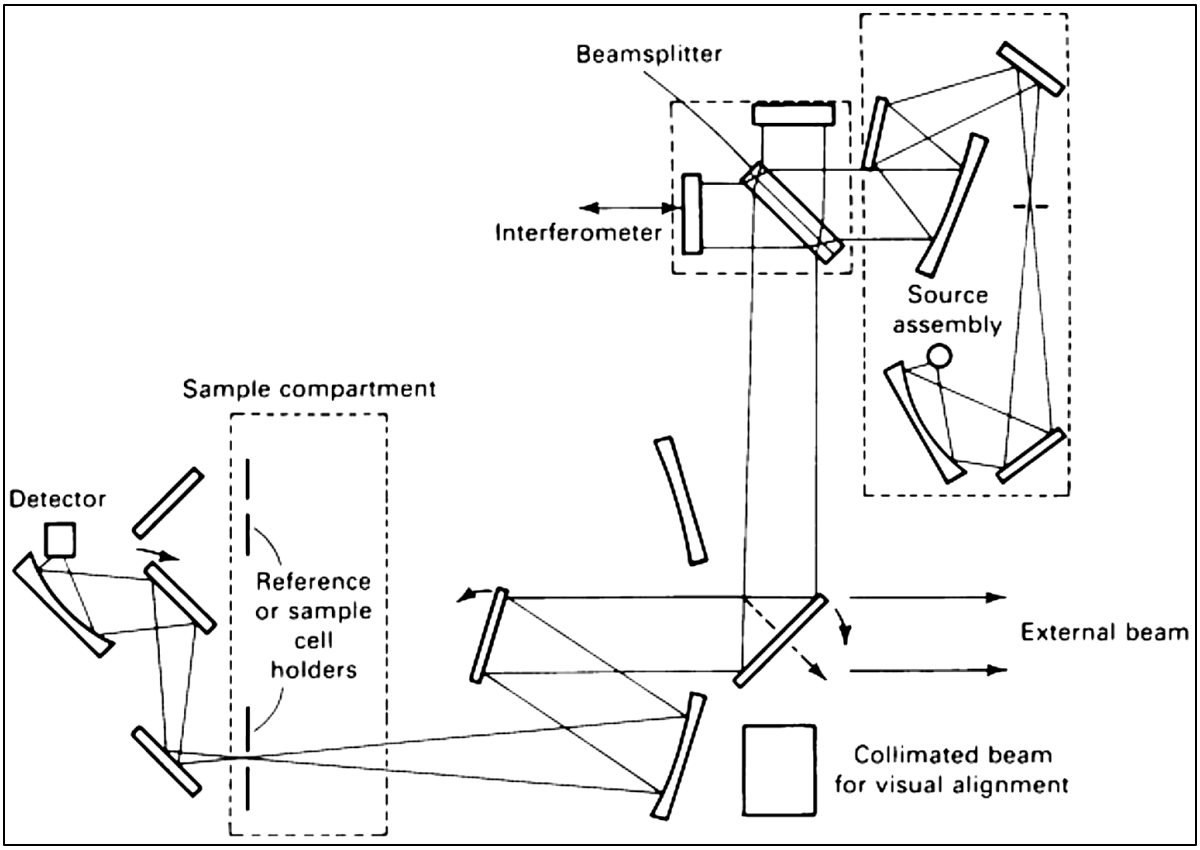

Fig. 2.2 Optical diagram of a FTIR spectrometer Courtesy of Digilab

2.3.2 Atomic Force Microscope (AFM)

It reveals about the thickness and the texture of the film. Atomic Force Microscopy (AFM) is a very high-resolution type of scanning probe microscopy, with demonstrated resolution on the order of fractions of a nanometer, more than 1000 times better than the optical diffraction limit. The AFM is one of the foremost tools for imaging, measuring, and manipulating matter at the nano scale and hence can be used for the LB films. The information is gathered by feeling the surface with a mechanical probe. Piezoelectric elements that facilitate tiny but accurate and precise movements on (electronic) command enable the very precise scanning. In some variations, electric potentials can also be scanned using conducting cantilevers. In newer more advanced versions, currents can even be passed through the tip to probe the electrical conductivity or transport of the underlying surface, but this is much more challenging with very few groups reporting reliable data [5-7].

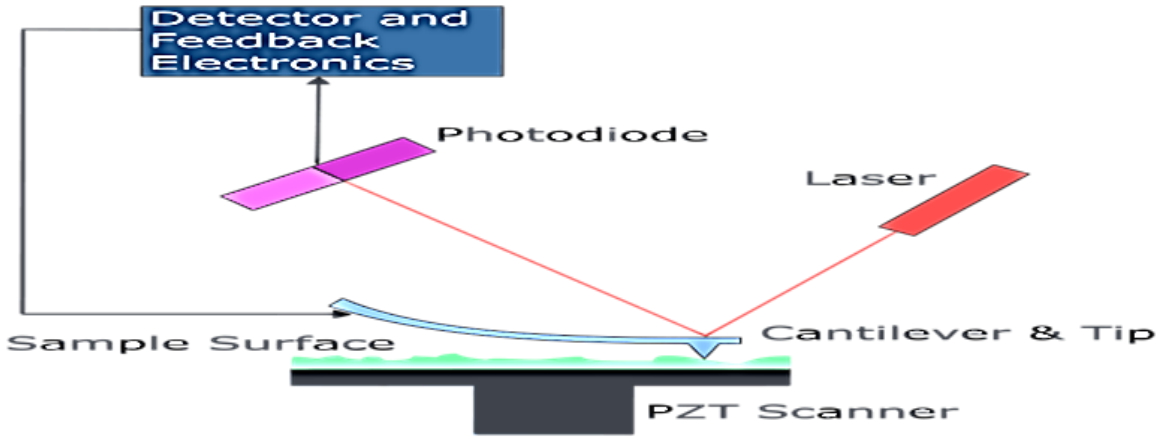

Fig. 2.3 Electron micrograph of a used AFM cantilever image width ~100 micrometers and ~30 micrometers

2.3.2.1 Basic Principle of AFM

The AFM consists of a cantilever with a sharp tip (probe) at its end that is used to scan the specimen surface. The cantilever is typically silicon or silicon nitride with a tip radius of curvature on the order of nanometers. When the tip is brought into proximity of a sample surface, forces between the tip and the sample lead to a deflection of the cantilever according to Hooke's law. Depending on the situation, forces that are measured in AFM include mechanical contact force, vender Waals forces, capillary forces, chemical bonding, electrostatic forces, magnetic forces (magnetic force microscope). Along with force, additional quantities may simultaneously be measured through the use of specialized types of probe. Typically, the deflection is measured using a laser spot reflected from the top surface of the cantilever into an array of photodiodes. If the tip was scanned at a constant height, a risk would exist that the tip collides with the surface, causing damage. Hence, in most cases a feedback mechanism is employed to adjust the tip-to-sample distance to maintain a constant force between the tip and the sample. Traditionally, the sample is mounted on a piezoelectric tube that can move the sample in the z direction for maintaining a constant force, and the x and y directions for scanning the sample. Alternatively a 'tripod' configuration of three piezo crystals may be employed, with each responsible for scanning in the x, y and z directions. This eliminates some of the distortion effects seen with a tube scanner. In newer designs, the tip is mounted on a vertical piezo scanner while the sample is being scanned in X and Y using another piezo block. The resulting map of the area s = f (x, y) represents the topography of the sample.

The AFM can be operated in a number of modes, depending on the application. In general, possible imaging modes are divided into static (also called contact) modes and a variety of dynamic (non-contact) modes where the cantilever is vibrated.

2.4 Reference

1. Chechel O.V. and Nikolaev E.N., Instruments and Experimental Techniques, 750, **34**, (1991).
2. Connes J. and Connes P., Journal of the Optical Society of America, 896, **56**, (1966).
3. Prati S., Joseph E., Sciutto G. and Mazzeo R., Accounts of Chemical Research, 792, **43**, (2010).
4. Beauchaine J.P., Peterman J.W. and Rosenthal R.J., Microchimica Acta, 133, **94**, (1988).
5. Lang K.M., Hite D.A., Simmonds R.W., McDermott R., Pappas D.P., and Martinis J.M., Review of Scientific Instruments, 2726, **75**, (2004).
6. Giessibl and Franz J., Reviews of Modern Physics, 949, **75**, (2003).
7. Roiter Y. and Minko, Journal of the American Chemical Society, 15688, **127**, (2005).

CHAPTER – 3

3.1 Liquid Crystals

There are five common states of matter are: solid, liquid, gas, liquid crystal and plasma. Liquid crystal is a fourth state that certain kinds of matter can enter into under the right conditions. The molecules in solids exhibit both positional and orientational order. In other words, the molecules are constrained to point only certain directions and to be only in certain positions with respect to each other. In liquid, the molecules do not have any positional or orientational order. The direction the molecules point and their positions are random.

The liquid crystal phase exists between the solid and the liquid phase. The molecules in liquid crystal do not exhibit any positional order, but they do possess a certain degree of orientational order. The molecules do not all point the same direction all the time. They merely tend to point more in one direction over time than other directions. This direction is referred to as the director of the liquid crystal.

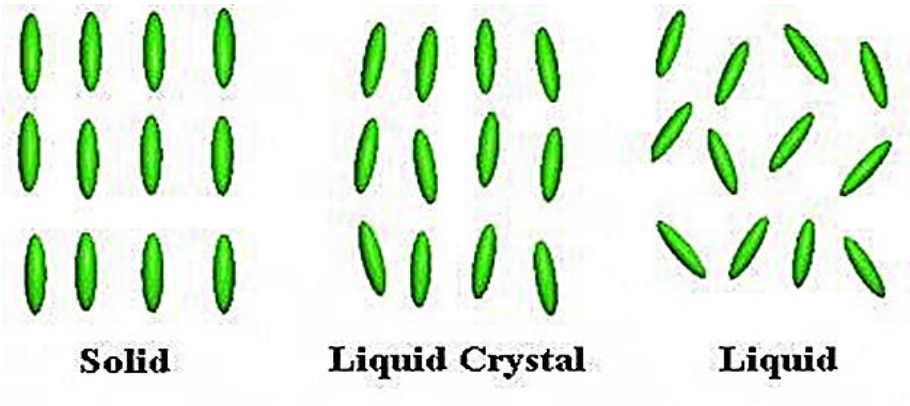

Fig. 3.1 Different type of states of matter

3.2 Characterizing Liquid Crystals

Each of these parameters describes the extent to which the liquid crystal sample is ordered. The following parameters describe the liquid crystalline structure:

- **Positional order** refers to the extent to which an average molecule or group of molecules shows translational symmetry (as crystalline material shows).
- **Orientational order** as discussed above represents a measure of the tendency of the molecules to align along the director on a long-range basis.

- **Bond Orientational Order** describes a line joining the centers of nearest neighbour molecules without requiring a regular spacing along that line. Thus, a relatively long-range order with respect to the line of centers but only short range positional order along that line.

3.3 Liquid Crystal Phase

3.3.1 Nematic Phase

The simplest liquid crystal phase is called the nematic phase (N). It is characterized by a high degree of long range orientational order but no translational order. Molecules in a nematic phase spontaneously order with their (for calamitic molecules) long axes roughly parallel. A schematic diagram of a nematic phase is shown in Fig. 3.2.

A uniformly aligned nematic has a preferred direction, often described in terms of a unit vector called the director. More generally a bulk nematic will contain domains. The orientation of the director is constant in each domain but is different in different domains. Viewed under a polarizing microscope the defect regions linking these domains appear as dark threads [1].

Nematics have fluidity similar to that of ordinary (isotropic) liquids but they can be easily aligned by an external magnetic or electric field. Aligned nematics have the optical properties of uniaxial crystals and this makes them extremely useful in liquid crystal displays (LCD) [2].

Fig. 3.2 Alignment in a nematic phase

3.3.2 Smectic Phase

The smectic phases which are found at lower temperatures than the nematic, form well-defined layers that can slide over one another in a manner similar to that of soap. The smectics are thus positionally ordered along one direction [3-4].

In the simplest smectic phase, the smectic-A (SmA) phase, the molecules order into layers with the layer normal parallel to the direction.

Closely related to the Smectic-A (SmA) phase is the smectic-C (SmC) phase. Here the molecules form a layer structure but the long axes of the molecules and hence the director lies at an angle to the layer normal as shown in fig. 3.3.

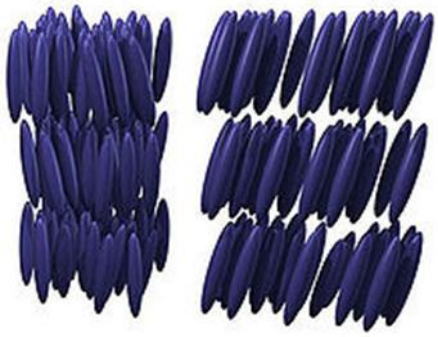

Fig. 3.3 Smectic A phase (left) has molecules organized into layers. In the smectic C phase (right), the molecules are tilted inside the layers

3.3.3 Chiral Phase

Chiral molecules can also form nematic phases called chiral nematic (cholesteric) phases (N*). This phase shows nematic ordering but the preferred direction rotates throughout the sample. The axis of this rotation is normal to the director. An example of chiral phase is shown in Fig. 3.4. The distance over which the director rotates by 360^0 is called the chiral pitch and is generally of the order of hundreds of nanometers and wavelength of visible light.

Fig. 3.4 The chiral nematic phase (left), also called the cholesteric phase, and the smectic C* phase (right)

A non-chiral nematic phase can be thought of as a chiral nematic with an infinite pitch. In the smectic C* phase (an asterisk denotes a chiral phase), the molecules have positional ordering in a

layered structure (as in the other smectic phases), with the molecules tilted by a finite angle with respect to the layer normal [5-6].

3.4 Properties of Liquid Crystals

Liquid crystal displays (LCD) offer several advantages over traditional cathode-ray tube displays. LCD's are flat and they use only a fraction of the power required by CRT's.

They are easier to read and more pleasant to work with for long periods of time than most ordinary video monitors. One should also now that there are several trades off, such as limited view angel, brightness and contrast, not to mention high manufacturing costs. As research continues, these limitations are slowly becoming less significant.

Today LCD's come mostly in two flavors passive and active. The less expensive passive matrix displays trade off picture quality, view angel, response time with power requirements and manufacturing costs. Active matrix displays have superior picture quality and viewing characteristics but need more power to run and are much more expensive to fabricate. Liquid crystal displays show great potential for the future and there are improvements to be made.

3.5 Literature Review

Sr. no.	Year	Name of author and title	Liquid crystal used	Characterization Techniques	Result
1.	1994	Barberot G. and et al. **Nematic liquid crystal anchoring on Langmuir-Blodgett Ws: steric, biphilic, dielectric and flexoelectric aspects and instabilities [7].**	E7	Electric and Geometrical study (by Theoretical Measurements)	Different aspects of geometrical and electrical roughness of LB film treated surfaces and quantifying them in terms of steric, dielectric, gradient flexoelectric and ordoelectric interactions, a general theoretical framework for NLC anchoring on LB films.

2.	1995	West J.L. and et al. **Dichroic ultraviolet absorption of thin liquid crystal films [8].**	E7	Spin coating and UV spectroscopy	Liquid crystal films were prepared by spin coating solutions of E7 in hexane on the plates. Thickness was controlled by varying the concentration of the E7 solution (0.05%– 4.0%) by weight as well as the spin speed ~2000–4000 rpm. Cyanobiphenyl liquid crystals absorb strongly in the ultraviolet. UV absorption spectra for parallel and perpendicular orientations of a thin E7 film. Absorbance peaks for both orientations were near 290 nm.
3.	1999	Corvazier L. and et al. **Induction of Liquid Crystal Orientation through Azobenzene Containing Polymer Networks [9].**	E7	UV Polarization	A diacrylate monomer containing a core of azobenzene groups was synthesized and liquid crystals stabilized by an azobenzene-containing polymer network. Linearly polarized UV irradiation is applied on thin films at room temperature shows the alignment of azobenzene groups on the network.
4.	2000	Zemek J. and et al. **CNx films created**	E7	FTIR Spectroscopy	FTIR and Raman spectra analysis revealed a complex

		by combined laser deposition and r.f. discharge: XPS, FTIR and Raman analysis [10].		and Raman Spectra	bonding structures based on a curve fitting of the N 1s spectra, and the N-sp^3 C, N-sp^2 C and N-H bonding states of nitrogen atoms were identified.
5.	2000	Zhao Y. and et al. **Liquid Crystalline Anisotropic Gels Prepared from Optical Alignment: Polymer Network Formed in the Isotropic Phase [11].**	E7	UV spectra and SEM	The UV spectra were recorded at room temperature after the film was subjected to a heating-cooling cycle in the absence of irradiation. The incident beam was polarized parallel and perpendicular to the polarization direction of the irradiation for alignment. SEM pictures (top view) for both irradiated and non-irradiated areas. The fiber like azobenzene network in the irradiated area is indeed aligned perpendicular to the polarization direction, while no alignment can be noticed for the non-irradiated area.
6.	2000	Guan L. and et al. **Self-Assembly of a Liquid Crystalline Anisotropic Gel [12].**	E7	Sol Gel Method and SEM	A new azobenzene-containing gelator AG1 is able to gel E7 nematic liquid crystal. A thin films cast on glass slides, the formation of intermolecular hydrogen bonds is allowed to proceed at temperatures close to the sol gel phase transition temperature. This self-assembly

					process leads to the formation of a macroscopically oriented H-bonded network in the liquid gel, which, in turn, can induce a long-range LC orientation in the LC gel state. SEM micrographs show the morphology of thin film of E7.
7.	2002	Rafferty D.W. and et al. **Fourier Transform Infrared Imaging of Nematic Liquid Crystals [13].**	E7	FTIR Spectroscopy	FT-IR spectroscopy is used to study the nematic liquid crystal. The strong dependence of the IR absorption of nematic liquid crystals on the alignment and ordering is important to consider for the interpretation of FT-IR images. The effect of ordering and combined effects of ordering and alignment for E7 were found to cause reductions in the nitrile band height of 28.7 and 65.0%, respectively.
8.	2004	Z. F. Li and et al. **Luminescent Silicon Nanoparticles Capped by Conductive Polyaniline through the Self-Assembly Method**	Silicon nano-particle and PANI	self-assembled method, XRD, FTIR spectroscopy	SiO_2 nanoparticles were successfully capped with polyaniline through reaction with a self-assembled bromopropyl silane monolayer. The composition, structure, morphology, and other physical properties of the PANI-capped Si nanoparticles were examined

		[14].			by X-ray photoelectron spectroscopy, Fourier transform infrared spectroscopy, and X-ray diffraction, which proved that polyaniline was grafted onto the surface without affecting the crystallinity of the silicon nanoparticles.
9.	2005	Tsai T. Y. and et al. **Electro-optical properties of a twisted Nematic – montmorillonite-clay nanocomposite [15].**	E7	XRD	The x-ray diffraction (XRD) profile of pure E7. There are two signals, with one at $2\theta = 3.36^{\circ}$ and the other at 20.44°.
10.	2008	Lin Y. H. and et al. **Electrically tunable wettability of liquid crystal/polymer composite films [16].**	E7	AFM	Electrically tunable wettability of an E7 LC/polymer composite film in which E7 NLC molecules are anchored among polymer grains. NLC reorientation among polymer grains at the LC/polymer composite film surfaces which are switched by the electric field. The AFM images of the surface of the LC/polymer films shows elongated aggregation of polymer grains along the rubbing direction

11.	2008	Zou H. and et al. **Polymer/Silica Nano composites: Preparation, Characterization, Properties and Applications [17].**	Silicon nano-Particle	Blending, Sol Gel and Polymerization	Preparation, characterization, properties, and application of polymer/silica nanocomposites. Three method for preparation can be used, blending, the sol-gel process and in situ polymerization.
12.	2010	Malihe Pishvaei and et al. **Synthesis of High Solid Content Polyacrylate/Nano s-ilica Latexes via Miniemulsion Polymerization [18].**	Silicon nano-Particle	Miniemulsion Polymerization and FTIR Spectra	High solid content nanocomposites of silica/acrylate polymer have been prepared by miniemulsion polymerization in semi-continuous operation. Different techniques for the characterization of the nanoparticles show that silica nanoparticles are well located in the polymeric structure.

3.6 REFERENCE

1. Gennes P. G., ***Physics of Liquid Crystals***, Publisher: Academic press, (1976).
2. Tanggaard A.T., Lara S., Danny N., Jesper L., Johannes W., Lei W., Giovanni T. and Paolo B., Optical and Quantum Electronics, 12, 39, (2007).
3. Gennes, P.G. and Prost, ***Physics of Liquid Crystals***, Publisher: Clarendon Press, (1993).
4. Chandrasekhar S., ***Liquid Crystals***, Publisher: Breach Science press, (1997).
5. Dierking I., Wiley-VCH, 527, **3**, (2003).
6. Kopp V. I., Fan B., Vithana H. K. M. and Genack A. Z., Journal of Optics Letters, 1707, 23, (1998).
7. Barberot G. and Petrovf A.G., Journal of Physics Condense Matter, 2291, **6**, (1994).

8. West J.L., Magyar G.R., Kelly J.R., Kobayashi S., Iimura Y., and Yoshida N., Applied Physics Letter, 2, **67**, (1995)
9. Corvazier L. and Zhao Y., Macromolecules, 3195, **32**, (1999).
10. Jelinek M., Zemek J., Trchova M., Vorlicek V., Lancok V., Tomov R. and Simeckova M., Thin Solid Films, 366, **69**, (2000).
11. Zhao Y. and Chenard Y., Macromolecules, 5891, **33**, (2000).
12. Guan L. and Zhao Y., Chemistry of Material, 3667, **12**, (2000).
13. Rafferty D.W., Koenig J.L., Magyar G., and West J.L., Applied of spectroscopy, 284, **56**, (2002).
14. Li Z.F., Swihart M.T., and Ruckenstein E., Langmuir, 1963, **20**, (2004).
15. Tsai T.Y., Huang Y.P., Chen H.Y., Chang Y.M, and Chin W.K., Nanotechnology, 1053, **16**, (2005).
16. Lin Y.H., Ren H., Wu Y. H., Wu S.T., Zhao Y., Fang J. and Lin H.C., Optics Express, 22, **16**, (2008).
17. Zou H., Wu S. and Shen J., Chemical Reviews, 3893, **108**, (2008).
18. Pishvaei M. and Tabrizi F.F., Iranian Polymer Journal, 707, **19**, (2010).

CHAPTER-4

4.1 Materials used

We have deposited Langmuir Blodgett thin film of eutectic E7 liquid crystal. E7 is a mixture of alkyl- and alkoxycyanobiphenyls shown in Table 4.1 [1]. Each extreme right end of component (-CN group) gives hydrophilic character to E7 molecule and alkyl chain present at left end provide hydrophobic character. So, E7 has amphiphilicity in nature. It will form stable monolayer at air-water molecules and hydrophobic part will be lying in upward direction at air-water interface.

The molecular formula of eutectic E7 liquid crystal consists of four liquid crystals as below:

Liquid Crystal	Molecular formula	percentage of liquid crystal
5CB 4-n-penntyl-4 cyanobiphenyl	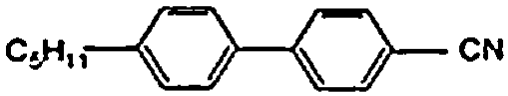	51%
7CB 4-n-heptyl-4-cyanobiphenyl	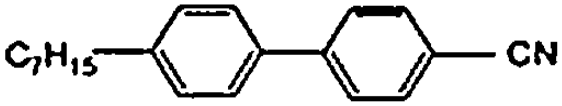	25%
8OCB 4-n- octoxy-4-cyanobiphenyl	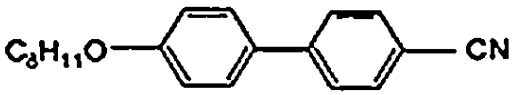	16%
5CT 4-n-pentyl-4-cyano-p-terphenyl	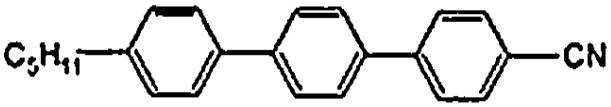	8%

Table 4.1 Four component eutectic E7 nematic liquid crystal mixture

Fig. 4.1 Phase Diagram of E7 showing nematic phase at room temperature

Langmuir Blodgett film was formed when molecules have amphiphilic character, so that molecules form stable monomolecular layers at the air-water interface. E7 nematic liquid crystal has amphiphilic molecule because of specific structure. The amphiphilic compound is dissolved easily in an evaporating solvent (chloroform) and spread at the water subphase in the Langmuir trough as shown in Fig. 4.2 (a).

The monolayer formed at the air-water interface can be transferred onto a solid substrate. The hydrophilic quartz substrate is used for transfer of monolayer.

As hydrophilic substrate is used so polar head group orients towards the substrate. As a result of the transfer, the surface of the substrate covered by the monolayer becomes hydrophobic shown in Fig. 4.2 (b).

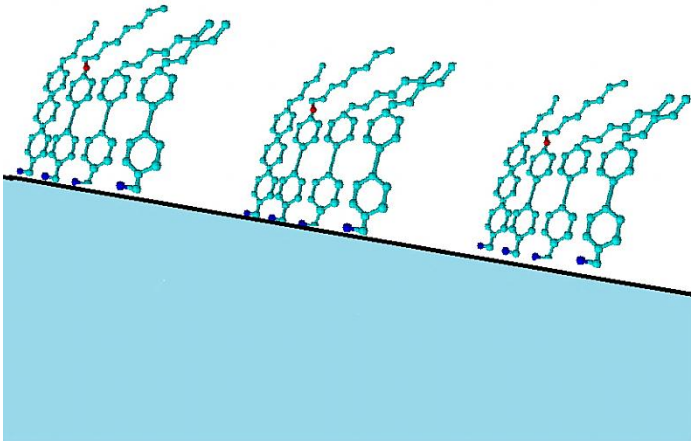

(a)

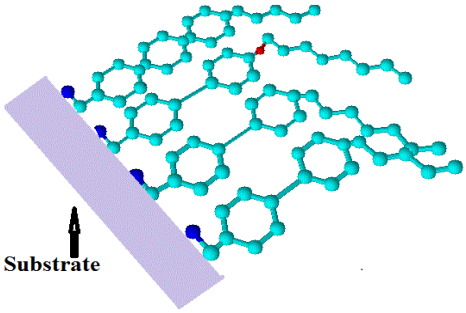

(b)

Fig. 4.2 (a) E7 nematic liquid crystal molecules on water Subphase, (b) monolayer deposited on quartz substrate

The chloroform (SDFCL, 99% purity) was used as solvent without further purification. SiO_2 nanoparticles (size 5-15 nm) (Sigma-Aldrich) was used as doping material, polyvinyl alcohol (PVA) (Merck) and Sodium dodecyl sulfate (SDS) (LOBA Chemie) were used for capping SiO_2 nanoparticle. As trough cleaning is very important for good film deposition. Trough was cleaned thoroughly before every experiment. Ethanol (Merck) was used to clean trough and after that trough as rinsed twice with deionized water. Barriers were also cleaned with ethanol. Wilhelmy plate was cleaned with ethanol, to ensure that no molecules of pervious monolayer had attached with plate. Wilhelmy plate measure the surface pressure of monolayer molecule. As we keep on compressing the barriers, surface pressure increases, because molecules come closer to each other.

We have deposited our Langmuir Blodgett films on quartz substrate. Quartz substrate was ultrasonicated in acetone (LOBA Chemie) for 15mins. Then it rinsed with deionized water.

4.2 Methodology

Preparation of E7 nematic liquid crystal composite 1mg/ml of E7 0.5mg was dissolved in 0.5 ml chloroform. Then water subphase was made from ultrapure milli-Q (ρ=18.2MΩ) and at pH =6. Purity of water surface was ensured by Wilhelmy plate. Initially when no material was spread then $\prod$=0.05 mN/m. It was confirmed that no other material is present on the surface of water. Then we spread 50µL above solution on water surface with help of Hamilton micro syringe. Then barriers were compressed at constant rate 10mm/min. Isotherm was recorded and it gave us surface pressure profile with changing mean molecular area. Then barriers were opened at very slow rate. Then cleaned quartz substrate was clamped in dipper. Dipper was moved slowly into water subphase and monolayers were deposited by using Y-type deposition.

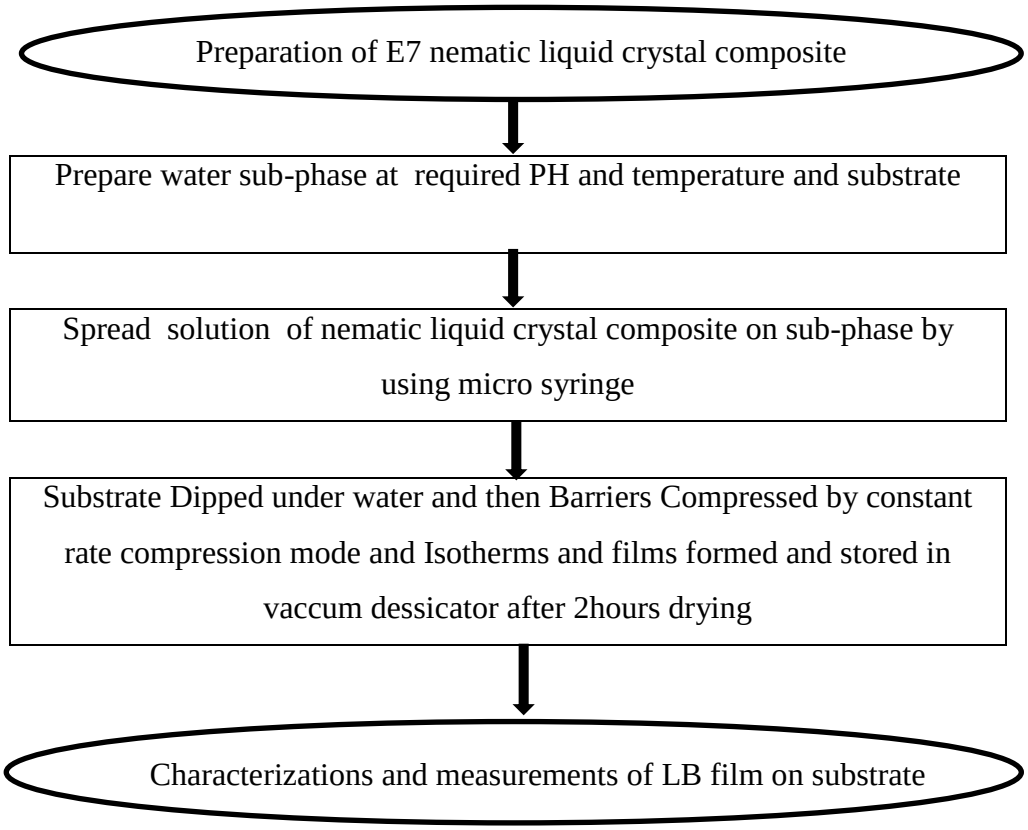

Fig. 4.3 Flow chart of methodology of preparation of Langmuir Blodgett Film

4.2.1 Need for capping of SiO_2 nanoparticles

SiO_2 nanoparticles do not form stable Langmuir Blodgett film, as they do not fulfill basic condition of "Amphiphilicity" for Langmuir Blodgett film formation. So, we need hydrophobic part attached with SiO_2 nanoparticles. SiO_2 nanoparticles were capped with polyvinyl alcohol using below written chemical procedure.

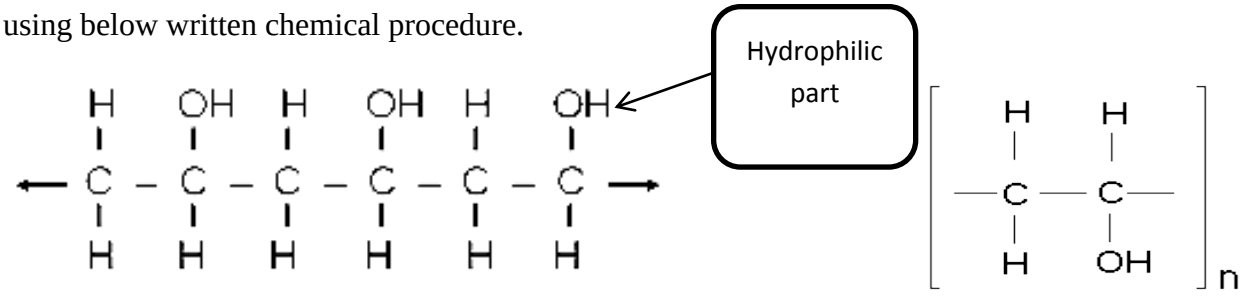

Fig. 4.4 Chemical formula of polyvinyl alcohol

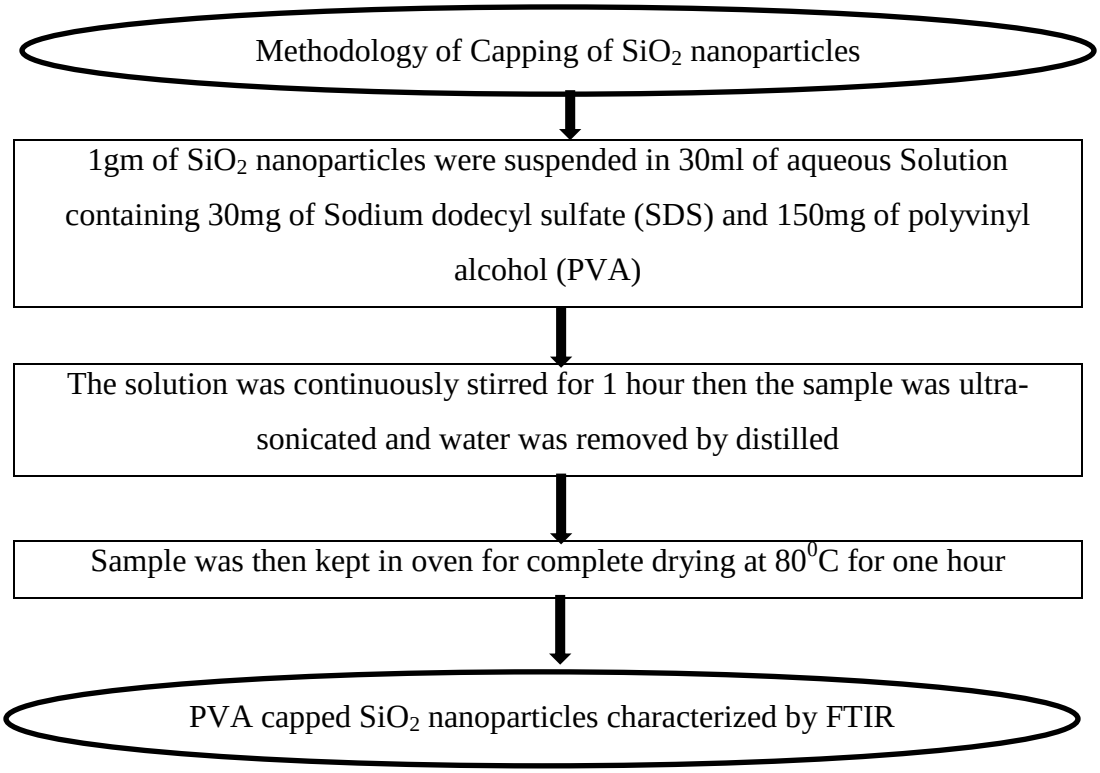

Fig. 4.5 Flow chart of methodology of capping of polyvinyl alcohol on SiO_2 nanoparticles

4.3 Characterization Techniques

4.3.1 Surface Pressure –Area Isotherm

The surface pressure (∏)-area (A) isotherm was recorded at air-water interface of KSV-NIMA

Mini Trough. We spread 100µl of E7 solution on air-water interface. Fig. 4.6 shows that ∏-A isotherm of the nematic liquid crystals, obtained during the compression. The monolayer was compressed symmetrically from both sides at a barrier motion speed of 10 mm/min. It was seen that nematic liquid crystal E7 was able to form a stable Langmuir Blodgett film [2]. Initially at mean molecular area Mma=75Å^2/molecule, barriers were far part and molecules had negligible surface pressure. As compression process, continued molecules started interacting with each other because barriers come closer and results in increase surface pressure value. As shown in isotherm from a to b, molecules move from gaseous phase to liquid expanded phase. With further increase in compression, molecules move to liquid compressed phase (b to c). After this, a solid phase was formed at ∏= 4.5mN/m. This phase was suitable for film deposition, because stable monolayer is formed at air-water interface.

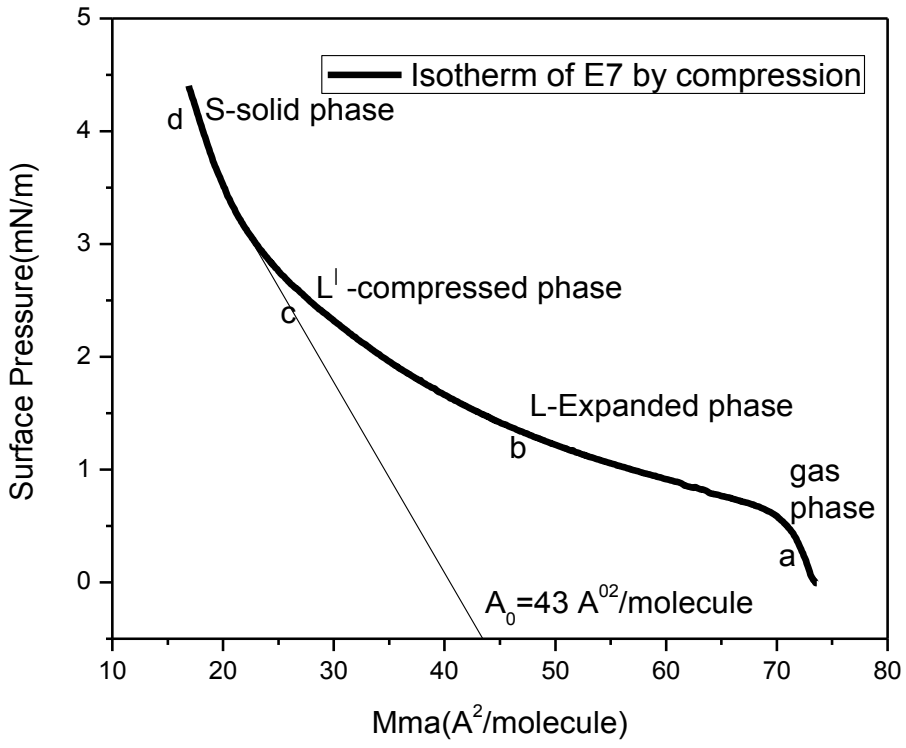

Fig. 4.6 Isotherm of pure E7 nematic liquid crystal

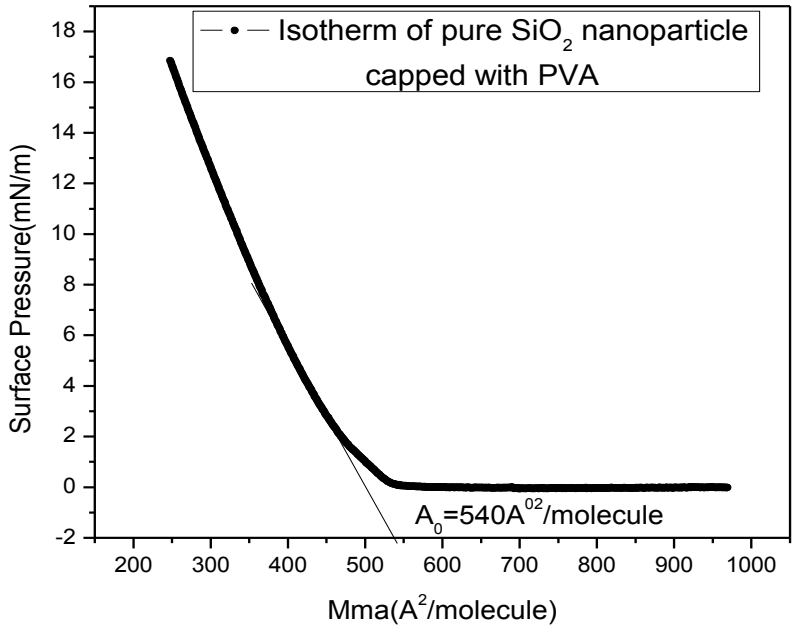

Fig. 4.7 Isotherm of pure polyvinyl alcohol capped SiO_2 nanoparticles

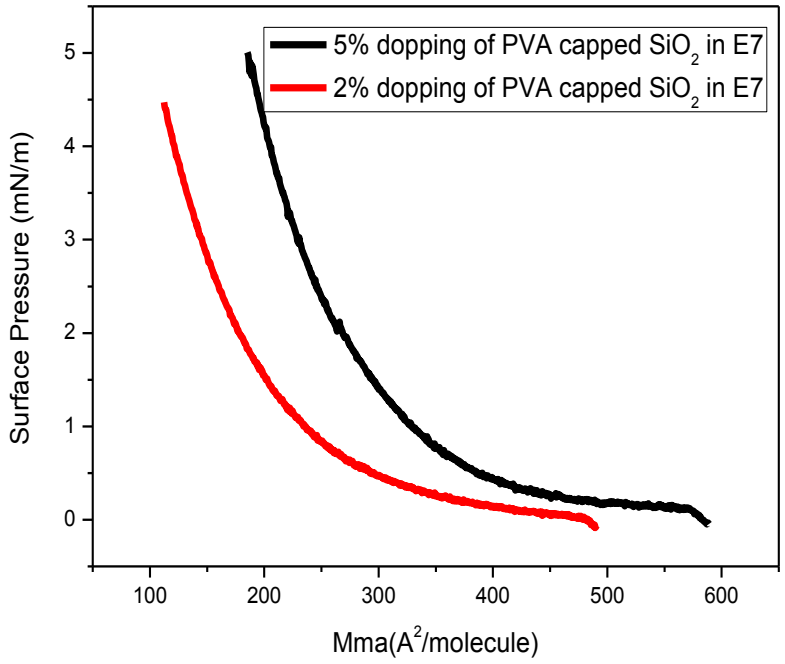

Fig. 4.8 Isotherms of 2% and 5% doping of PVA capped SiO_2 nanoparticles in E7.

Fig. 4.7 shows surface pressure-area isotherm of PVA capped SiO_2 nanoparticles dissolved in chloroform at 1mg/ml. 300µl of solution spreaded on air-water interface, 45 mins were provided for solvent to get volatile. Initially when barriers were far away then no interaction between PVA capped SiO_2 nanoparticles. Then at Mma ≈ 540$Å^2$/molecule, there was a sharp rise in surface pressure value. Molecules get aligned on water surface and formed a stable monolayer at≈16mN/m.

Fig. 4.8 shows isotherm profile for 2% and 5% doping of PVA capped SiO_2 nanoparticles by weight in E7 nematic liquid crystal. When we can clearly examine isotherm of these material, in case doping of 2% PVA capped SiO_2 nanoparticles in E7 have lesser mean molecular area as compared to 5% PVA capped SiO_2 nanoparticles in E7, because in 2% doping mixture have less weight composition of PVA capped SiO_2 nanoparticles, which results in lesser mean molecular area values. It can be clearly predicted that isotherm followed same phase sequence as it was in case of pure E7 nematic liquid crystal. Phase changes from gaseous to liquid phase and then to solid phase. Solid phase of 2% PVA capped SiO_2 nanoparticles in E7 mixture was attained at ∏=4.5mN/m, while 5% PVA capped SiO_2 nanoparticles in E7 was attained at ∏=5mN/m, which was higher than former one.

4.3.2 Hysteresis in Multiple Isotherms

Hysteresis was observed in pure E7 nematic liquid crystal multiple isotherms. When we repeat compression and expansion cycles, isotherm curves have hysteresis. This is because of mixed amphiphilic nature of E7 nematic liquid crystal molecules.

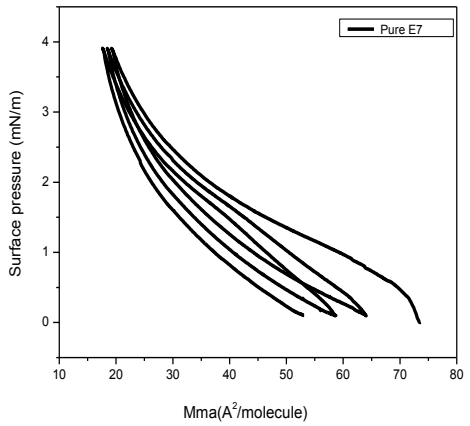

(a)

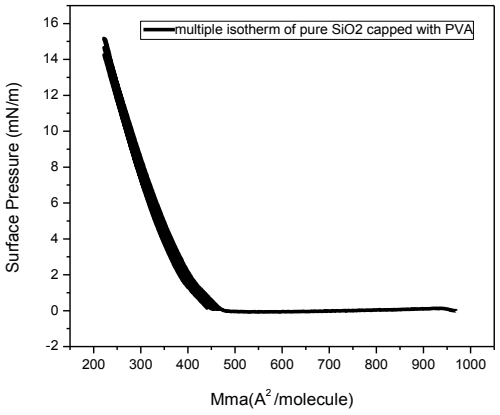

(b)

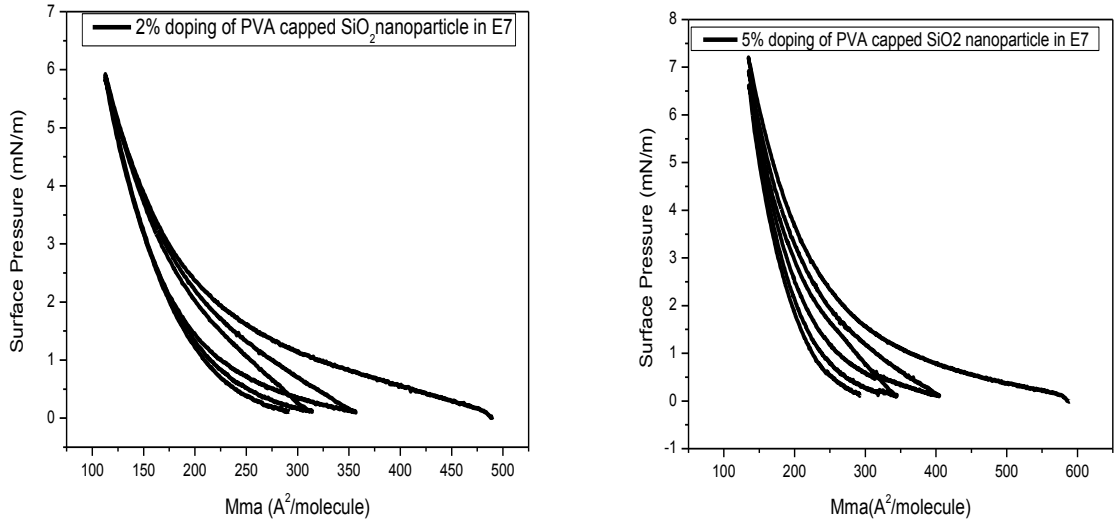

(c) (d)

Fig. 4.9 Multiple isotherms of (a) pure E7, (b) pure capped SiO_2 nanoparticle with PVA, (c) 2% doping of PVA capped SiO_2 nanoparticle in E7, (d) 5% doping of PVA capped SiO_2 nanoparticle in E7.

While PVA capped SiO_2 nanoparticles shows no hysteresis during isotherm cycles, because of elastic in nature. They retain their position when barrier pressure is removed.

In 2% doping of PVA capped SiO_2 nanoparticles in E7 and 5% doping of PVA capped SiO_2 nanoparticles, hysteresis is observed because larger amount of E7 nematic liquid crystal is present in these mixture [3-5].

4.3.3 Surface Pressure variation with time during multiple cycles Profile

Fig. 4.10 shows variation of surface pressure with time during three compression-expansion cycles. A similar trend was observed during each cycle (1, 2, 3). When we compressed barriers during first cycle surface pressure value increases up to 4mN/m, 15mN/m, 6mN/m and 7mN/m for pure E7, pure PVA capped SiO_2 nanoparticles, 2% doping PVA capped SiO_2 nanoparticles in E7 and 5% doping of PVA capped SiO_2 nanoparticles on E7 respectively. During each cycle monolayer reaches up to maximum surface pressure value. So we have three apex points during three cycles. Instead of having negligible hysteresis surface pressure varies in similar manner during each cycle [6].

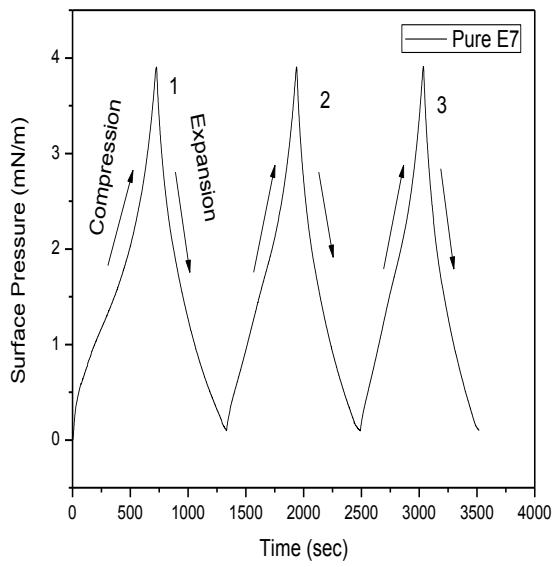

(a)

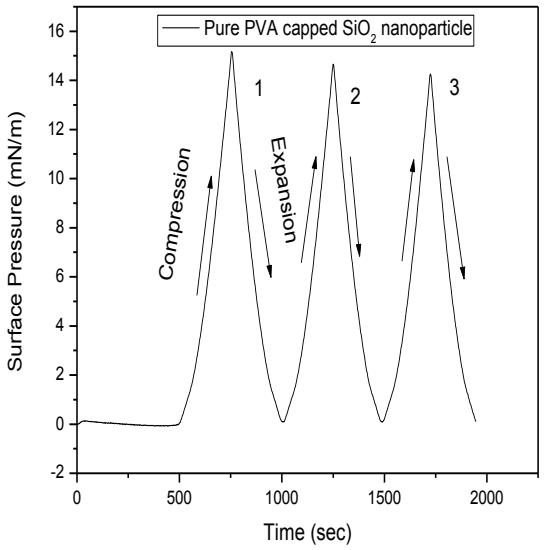

(b)

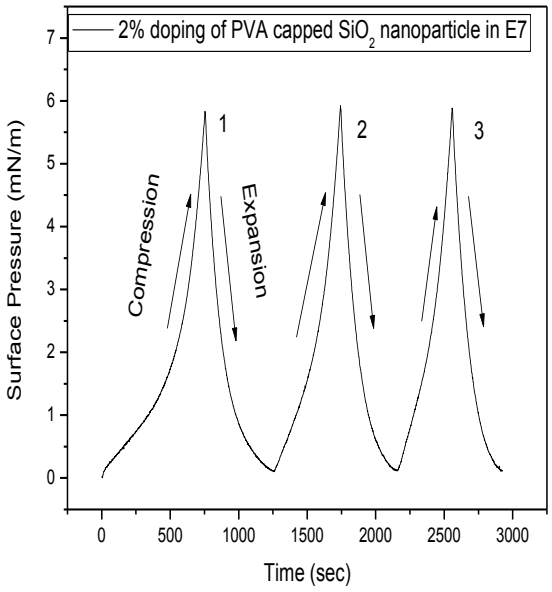

(c)

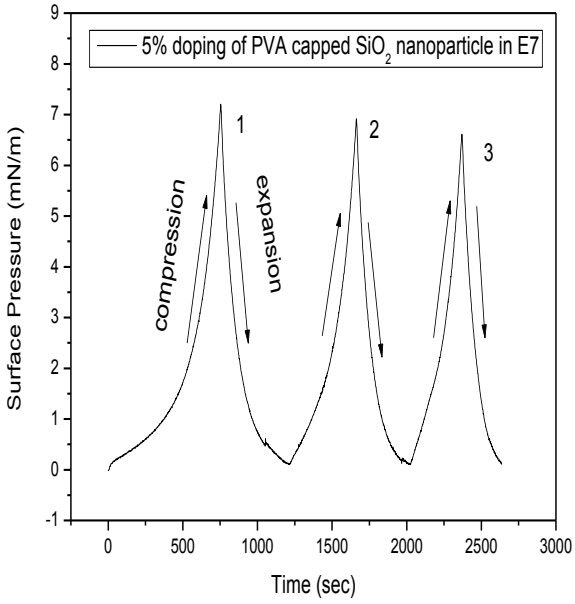

(d)

Fig. 4.10 Surface Pressure varies with time during multiple isotherms of (a) pure E7, (b) pure PVA capped SiO_2 nanoparticles, (c) 2% doping of PVA capped SiO_2 nanoparticles in E7 and (d) 5% doping of PVA capped SiO_2 nanoparticles in E7.

4.3.4 Stationary Elasticity Modulus

The Stationary elastic modulus E is an appropriate quantity for distinguishing very weak phase transitions. The elastic modulus is defined as

$$E = -(A_m)\, d\prod/dA_m$$

Where $d\prod/dA_m$ is change in surface pressure with A_m (mean molecules area), the elasticity (or compressing modulus) can be directly calculated from the slope of $\prod$-A isotherm.

Fig. 4.11 shows the variations of elastic modulus as a function of A_m during compression. In pure E7 when barriers are compressed then a sharp increase was observed in elasticity at value about Mma =70 $Å^2$/molecule because at that mean molecular area, molecules move from gaseous phase to liquid phase. Further compressed barrier, a continuous curves was obtained so almost horizontal line was observed with the E_s values of about 2-3mN/m. Similar Elasticity profile for PVA capped SiO_2 nanoparticles was observed but sharp peak was observed at about Mma=550$Å^2$/molecule then a horizontal line with E_s value of about 0mN/m was observed.

In 2% doping of PVA capped SiO_2 nanoparticles in E7 and 5% doping of PVA capped SiO_2 nanoparticles in E7, no sharp peaks were observed because isotherms of these composites were smooth, no sharp change in surface pressure with decrease with mean molecular area [7-8].

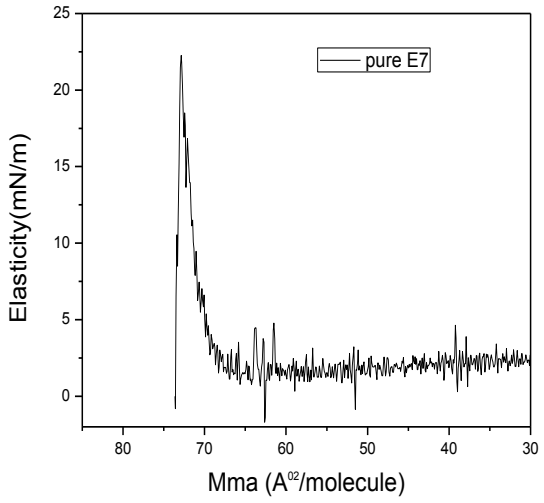

(a)

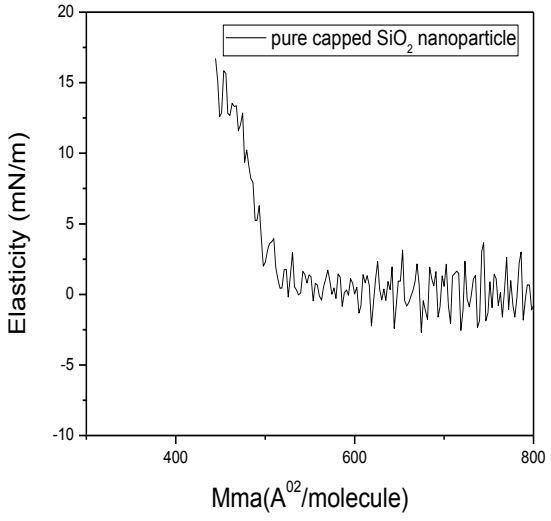

(b)

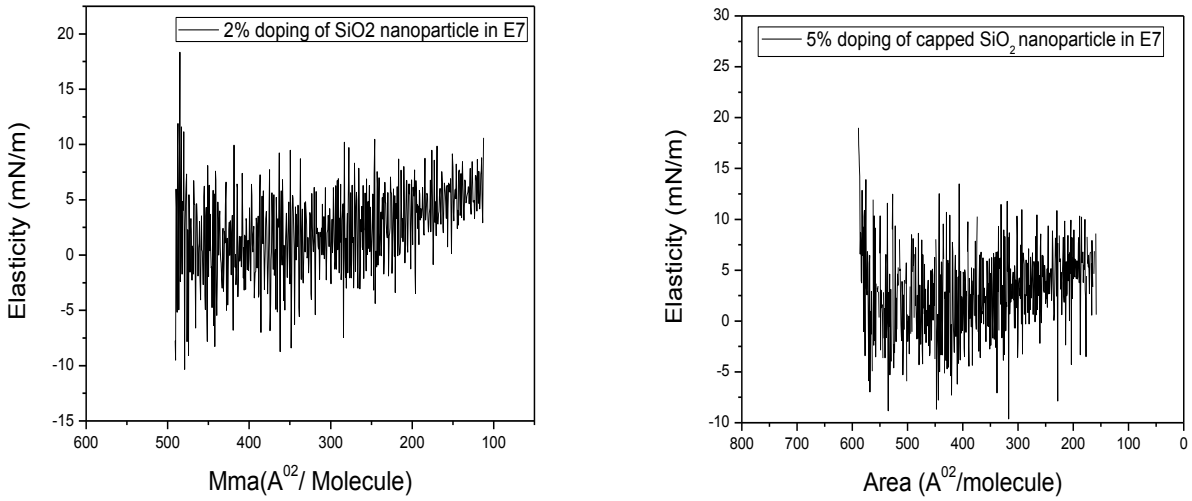

(c) (d)

Fig. 4.11 Stationary Elastic modulus of (a) pure E7, (b) pure PVA capped SiO_2 nanoparticle, (c) 2% doping of PVA capped SiO_2 nanoparticles in E7 and (d) 5% doping of PVA capped SiO_2 nanoparticle in E7.

4.3.5 Normalized Area-Time Profile

Fig. 4.12 shows normalized area vs time profile for pure E7, PVA capped SiO_2 nanoparticles, 2% and 5% doping of PVA capped SiO_2 nanoparticle in E7.

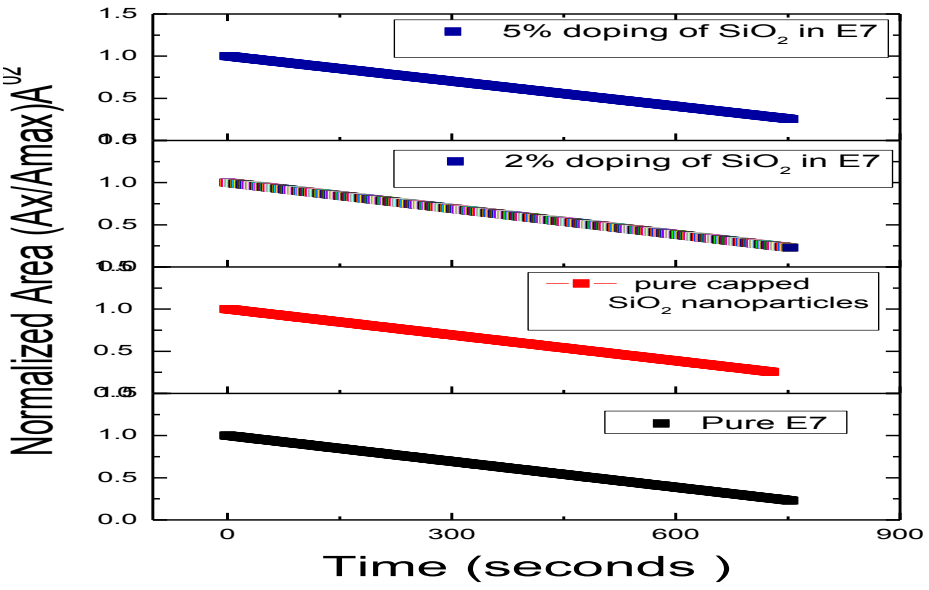

Fig. 4.12 Normalized Area-Time Profiles

Normalized Area= A_x/A_{max}

A_x represents mean molecular area during compression cycles. As we can clearly observed from profile of normalized area with time, it decreases constantly with time. Mean molecular area is decreasing, so molecules were coming close to each other which resulted in phase change during compression isotherm.

4.3.6 Equilibrium stabilized surface pressure during dipping process

Fig. 4.13 shows the equilibrium stabilized surface pressure during dipping process. When we deposit monolayer at quartz substrate, substrate was clamped into dipper and it was moved into the water surface. Isotherm plot was traced at beginning when monolayer get compressed up to target surface when dipping process was done, molecules moved from surface to the quartz substrate. Decrease in number of molecules will not result in decrease of surface pressure, because barriers automatically move forward and backward to attain a constant surface pressure. Deposition of pure E7 NLC was done at 3mN/m and 12mN/m was maintained constant during deposition of PVA capped SiO_2 nanoparticles.

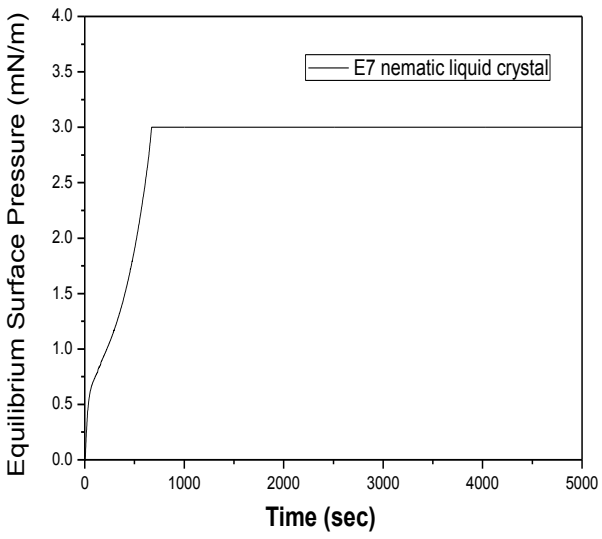

(a)

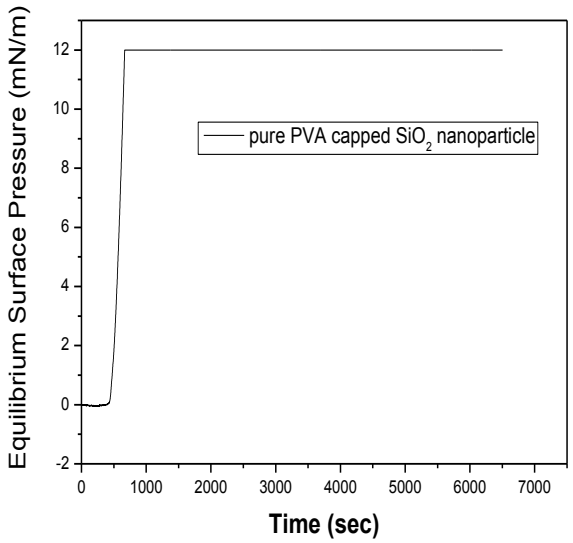

(b)

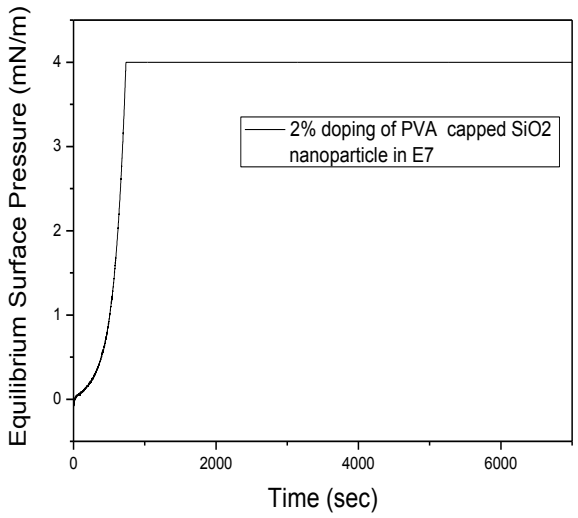

(c)

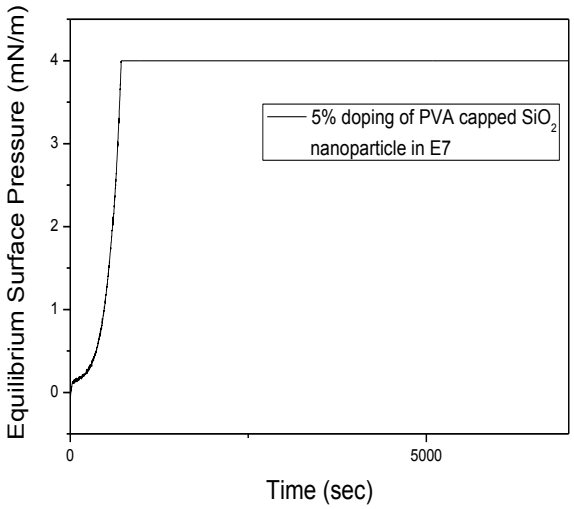

(d)

Fig. 4.13 Equilibrium stabilized surface pressure during dipping process of (a) pure E7, (b) pure PVA capped SiO_2 nanoparticle, (c) 2% doping of PVA capped SiO_2 nanoparticle in E7 and (d) 5% doping of PVA capped SiO_2 nanoparticle in E7.

2% doping of PVA capped SiO_2 nanoparticles in E7 and 5% doping of PVA capped SiO_2 nanoparticles in E7 were both deposited at surface pressure 4mN/m.

4.3.7 Atomic Force Microscopy (AFM)

Topography of monolayer was studied under NT-MDT (solver next) atomic force microscope. Silicon nitride (SiN) probe having tip curvature radius 2nm was attached to cantilever having resonance frequency (87-230 kHz), typical force constant 5.1mN/m, initially properly cleaned quartz substrate and root mean square roughness less than 1nm shown in fig. 4.14. It ensures that the smoothness of quartz substrate and suitable for monolayer deposition. E7 nematic liquid crystal was deposited on quartz substrate at 3mN/m and monolayer was attached to quartz substrate during dipping. Film was placed in vacuum desiccator to ensure moisture free film. Then it was analyzed under AFM.

Fig. 4.15 shows AFM of E7 monolayer in scan range $2\times2\mu m^2$. We observed uniform deposition throughout the range. Film roughness profile shows average particle size up to 4nm uniform pattern in height profile. 3D image shows uniformly aligned monolayer of E7 nematic liquid crystal molecules in Fig. 4.15 (c) [9].

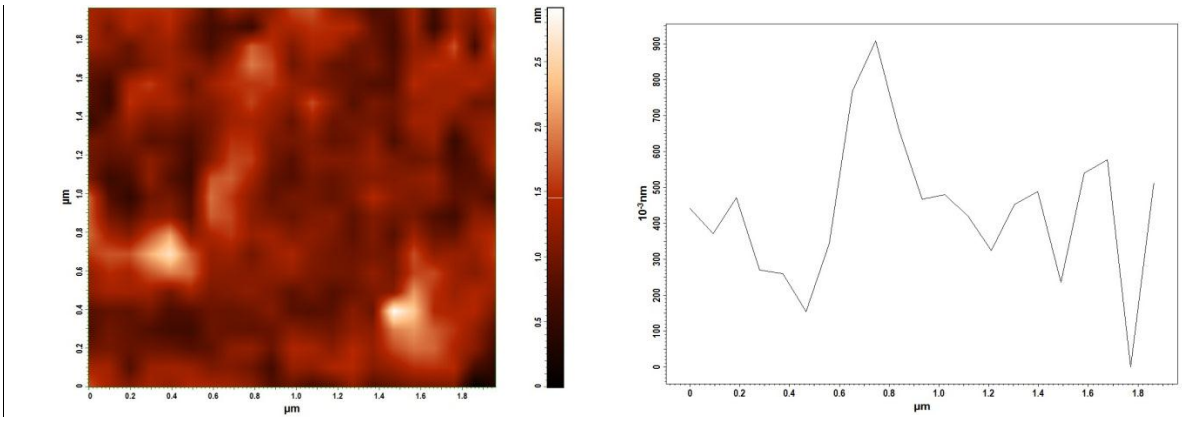

(a) (b)

Fig. 4.14 (a) Atomic Force Micrographs of clean quartz substrate in scan range 2×2μm^2, (b) Roughness profile

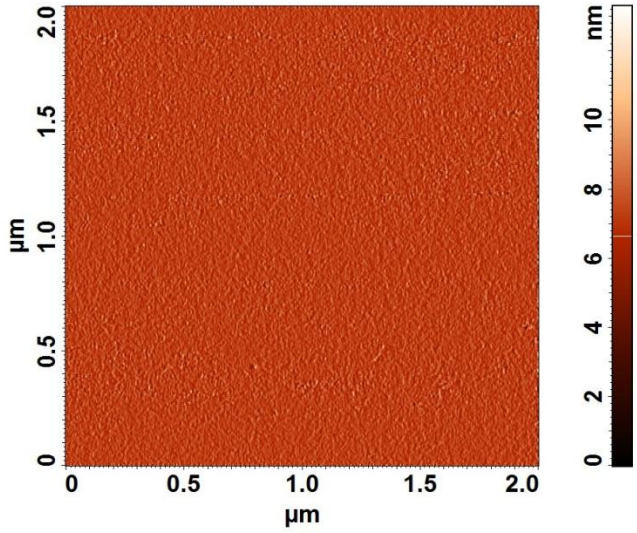

(a)

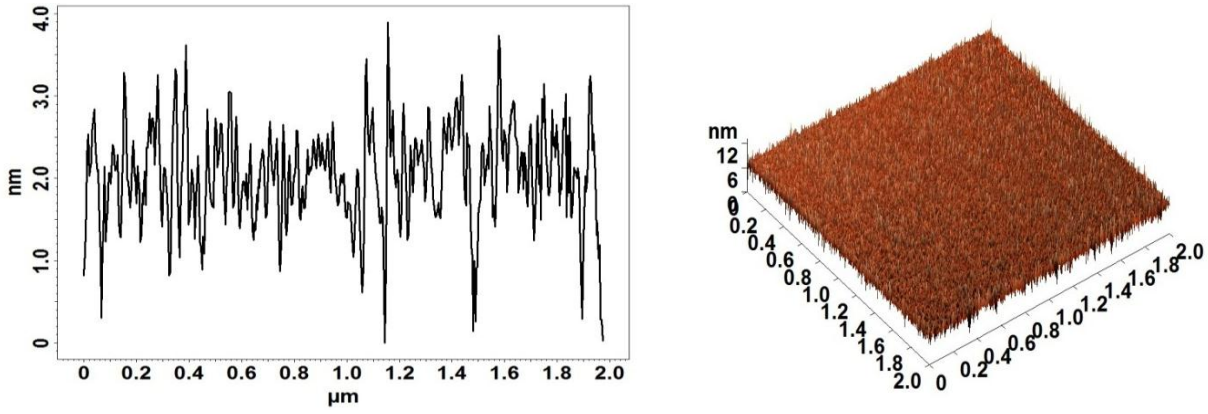

(b) (c)

Fig. 4.15 Atomic Force Micrographs of monolayer of E7 nematic liquid crystal on quartz substrate, (a) AFM images of the thin film in scan range 2×2μm^2, (b) roughness profile (c) 3D image.

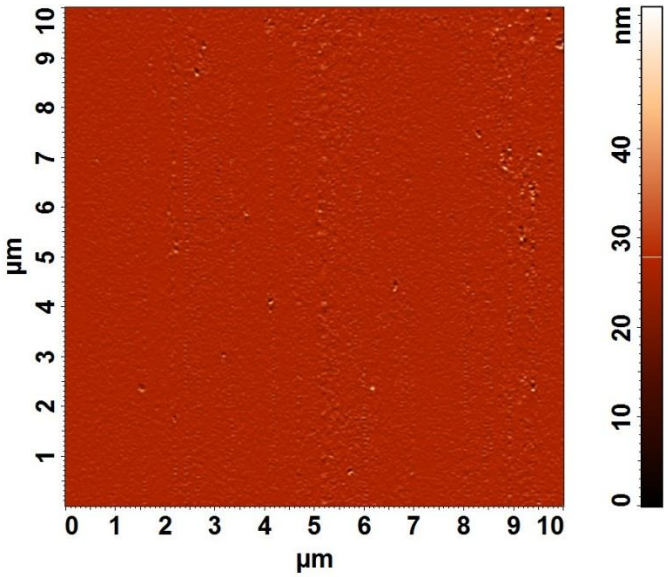

(a)

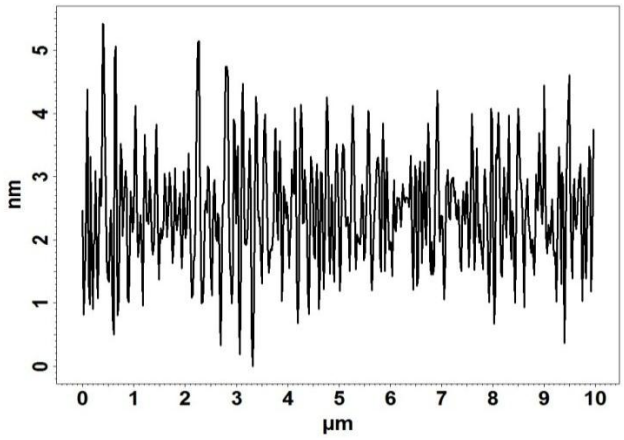

(b)

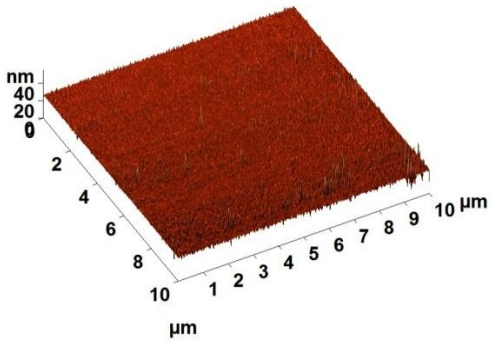

(c)

Fig. 4.16 Atomic Force Micrographs of monolayer of E7 nematic liquid crystal on quartz substrate, (a) AFM images of the thin film in scan range $10\times10\mu m^2$, (b) roughness profile, (c) 3D image.

Fig. 4.16 shows AFM of E7 monolayer in scan range $10\times10\mu m^2$. We observed the same uniform deposition throughout scan range as in $2\times2\mu m^2$ scan range. Average particle size up to 4nm shown in film roughness profile, 3D was shown uniform film deposited on quartz substrate in Fig. 4.16 (c).

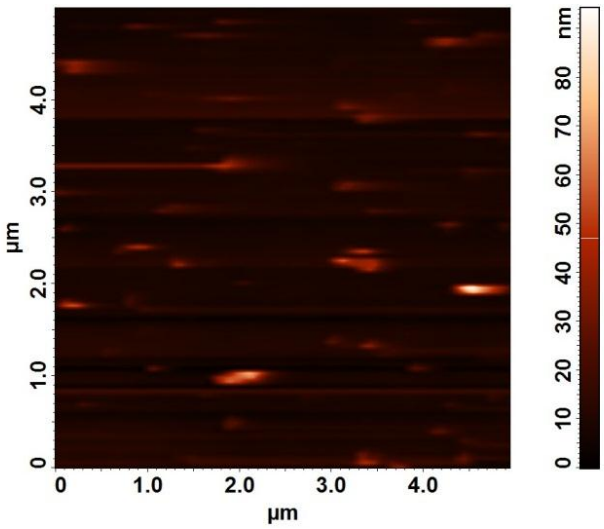

(a)

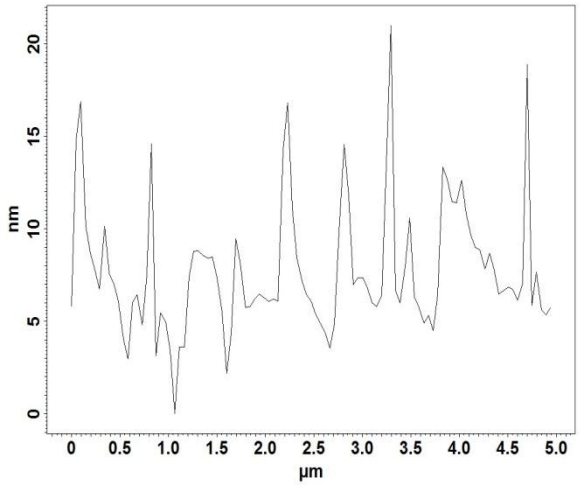

(b)

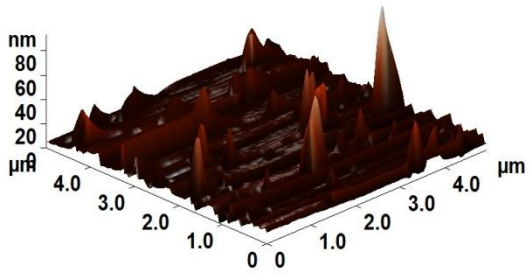

(c)

Fig. 4.17 Atomic Force Micrographs of monolayer of PVA capped SiO_2 nanoparticles, (a) AFM images of thin film in scan range $5\times5\mu m^2$, (b) roughness profile, (c) 3D image.

Fig. 4.17 shows the AFM images (5×5 μm^2) of polyvinyl alcohol (PVA) capped SiO_2 nanoparticles. Monolayer was transfer to quartz substrate at 12mN/m. Average particle size up to 20nm shown in film roughness height profile. Size of uncapped SiO_2 nanoparticles was about 5-10nm. After capping, the size of capped SiO_2 nanoparticles increased upto 20nm. Fig. 4.17 (c) shows 3D image of PVA capped SiO_2 nanoparticles [10].

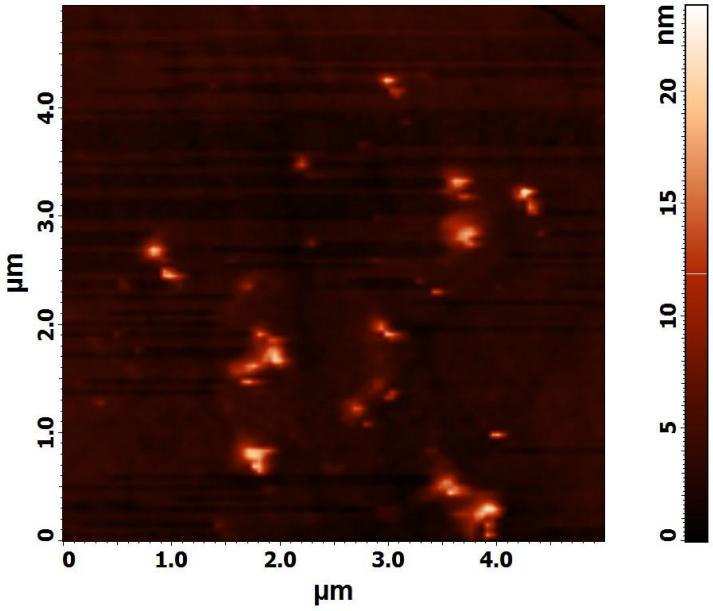

(a)

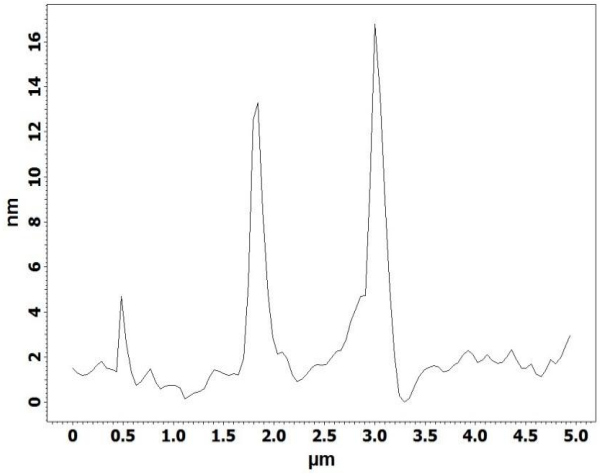

(b)

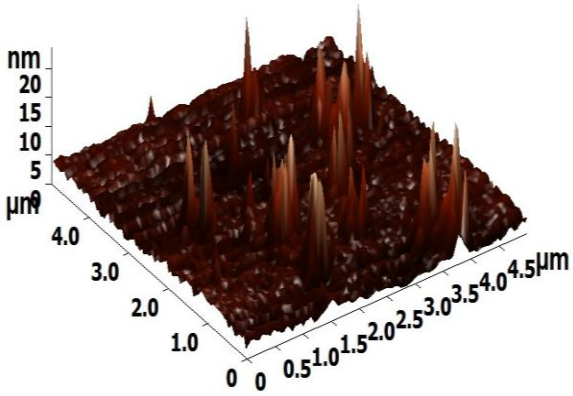

(c)

Fig. 4.18 Atomic Force Micrographs of monolayer of thin film of 2% doping of PVA capped SiO_2 nanoparticles in E7, (a) AFM images of the thin film in scan range $5\times5\mu m^2$, (b) roughness profile, (c) 3D image.

Fig. 4.18 shows the AFM image ($5\times5\mu m^2$) of 2% doping of PVA capped SiO_2 nanoparticles in E7. The monolayer of 2% doping of PVA capped SiO_2 nanoparticles was deposited on quartz substrate at 4mN/m. The average particle size upto 16-17 nm in height profile image. Fig. 4.18 (c) shows 3D image of PVA capped SiO_2 nanoparticles.

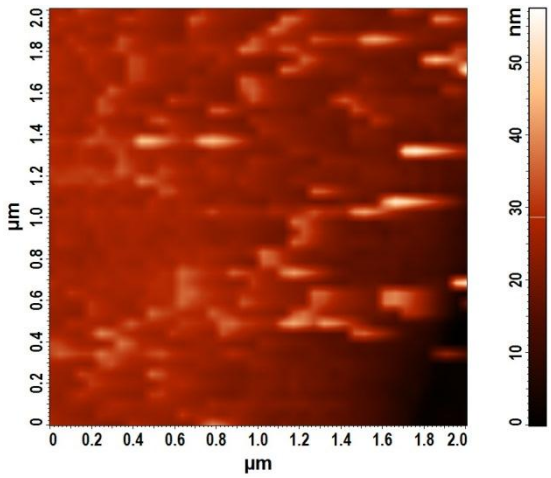

(a)

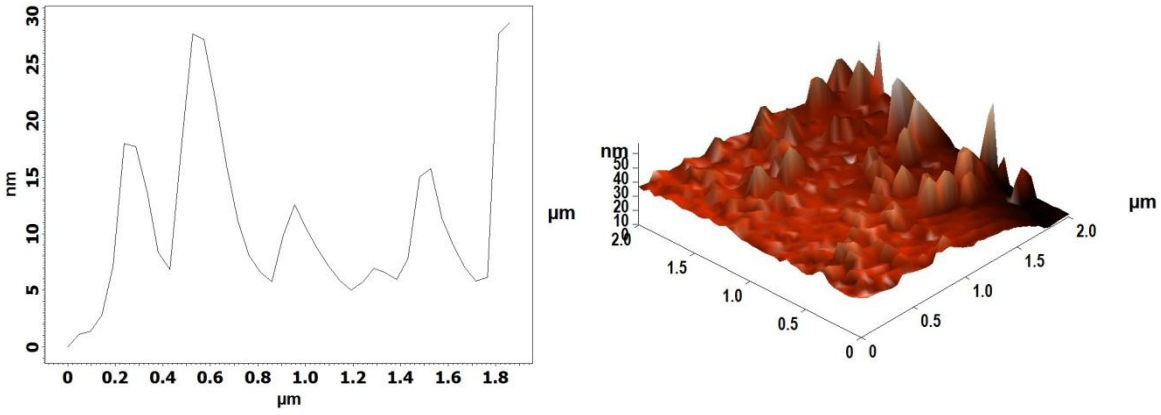

(b) (c)

Fig. 4.19 Atomic Force Micrographs of monolayer of thin film of 5% doping of PVA capped SiO_2 nanoparticles in E7, (a) AFM images of the thin film in scan range $2\times2\mu m^2$, (b) roughness profile, (c) 3D image.

Fig. 4.19 shows AFM images monolayer of 5% doping of PVA capped SiO_2 nanoparticles in E7 scan range $2\times2\mu m^2$. Monolayer of 5% doping of PVA capped SiO_2 nanoparticles in E7 deposited on quartz substrate at 4mN/m. It shows average particles size upto 30nm in height profile image. Fig. 4.19 (c) shows the 3D image of the 5% doping of PVA capped SiO_2 nanoparticles in E7.

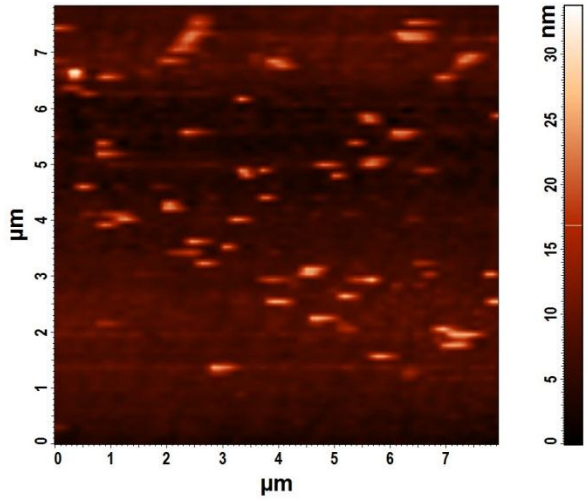

(a)

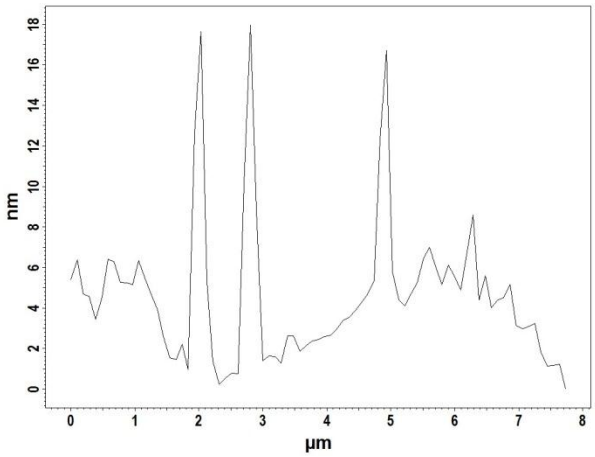

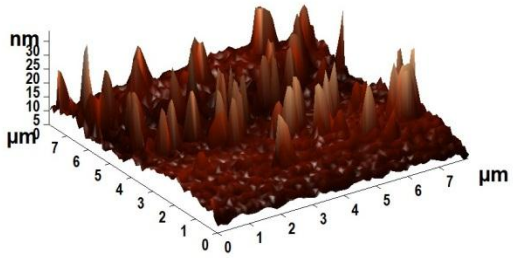

(b) (c)

Fig. 4.20 Atomic Force Micrographs of multilayers of 5% doping of PVA capped SiO_2 nanoparticles in E7, (a) AFM images of the thin film in scan range $8\times8\mu m^2$, (b) roughness profile, (c) 3D image.

Fig. 4.20 shows AFM images multilayer of 5% doping of PVA capped SiO_2 nanoparticles in E7 scan range $8\times8\mu m^2$. Multilayers of 5% doping of PVA capped SiO_2 nanoparticles in E7 deposited on quartz substrate at 4mN/m. It shows average particles size upto 18nm in height profile image. Fig. 4.20 (c) show as the 3D image of 5% doping of PVA capped SiO_2 nanoparticles in E7.

4.3.8 Fourier Transformation IR Spectroscopy (FTIR)

The FTIR transmittance spectra of SiO_2 nanoparticles, polyvinyl alcohol (PVA) and PVA capped SiO_2 nanoparticles are shown in Fig. 4.21.

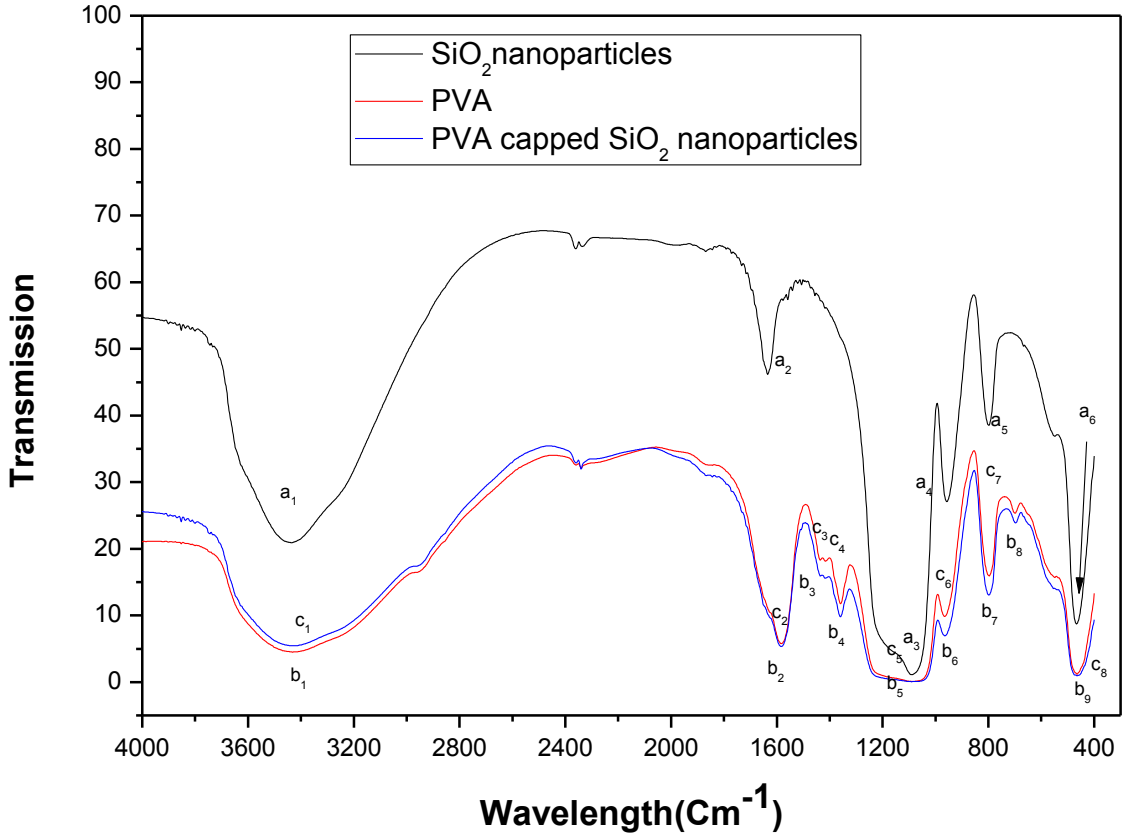

Fig. 4.21 FTIR transmission spectra of pure SiO_2 nanoparticles (black), Polyvinyl alcohol (PVA) (red) and PVA capped SiO_2 nanoparticles (blue)

Table 4.2 FTIR spectra of silicon dioxide (SiO_2) nanoparticles

a_1	3440 cm^{-1}	-OH stretching
a_2	1635 cm^{-1}	C-O bending
a_3	1083 cm^{-1}	Si-O-Si stretching
a_4	950 cm^{-1}	Si-O-H stretching
a_5	790 cm^{-1}	Si-O bending
a_6	456 cm^{-1}	Si-O out of plane deformation

The assignment of the bands in SiO_2 nanoparticles is shown in Table 4.2. The characteristic bands almost at 950, 790 and 456 cm^{-1} is correspond to the stretching, bending and out of plane of Si-O bonds, respectively. The main Si-O-Si stretching vibrational band at 1083 cm^{-1} shows silicon dioxide structure. Peaks at around of 1635 and 3440 cm^{-1} are attributed to vibrations of carbon and OH groups impurities atoms in the film [11-12].

Table 4.3 FTIR spectra of polyvinyl alcohol (PVA)

b_1	3420 cm^{-1}	-OH stretching
b_2	1559 cm^{-1}	C=C stretching
b_3	1447 cm^{-1}	CH_2 bending
b_4	1321 cm^{-1}	CH+OH stretching
b_5	1103 cm^{-1}	CO stretching
b_6	960 cm^{-1}	C-C stretching
b_7	798 cm^{-1}	CH_2, CH_3 stretching
b_8	694 cm^{-1}	OH stretching
b_9	456 cm^{-1}	

Different assignments of the bonds in polyvinyl alcohol (PVA) are shown in Table 4.3. The IR spectrum exhibits several bands characteristic of stretching and bending vibrations of O–H, C–H, C=C and C–O groups. Two bands are observed at 1321 and 694 cm^{-1} corresponding to the O–H stretching frequency, which indicate the presence of hydroxyl groups. One band observed at 1559 cm^{-1} has been assigned to C=C stretching mode. Two bands observed at 1447 and 798 cm^{-1} have been attributed to bending and stretching modes of CH group, respectively. A band at 1321 cm^{-1} has been assigned to the combination frequency of (CH + OH) group. The strong band at 1103 cm^{-1} and sharp band at 960 cm^{-1} have been attributed to the stretching mode of CO and C-C groups respectively [13].

Different assignments of the bonds in polyvinyl alcohol (PVA) capped SiO_2 composite are shown in Table 4.4. The IR spectrum exhibits several bands characteristic of stretching and bending vibrations of O–H, C–H, C=C and C–O, Si-O, Si-O-C groups. Different bands coming from stretching vibration of Si-O-Si bonds (1103 cm^{-1}) of silica and Si-O-C bonds (960 cm^{-1}) of

PVA. Three bands observed at 1559, 1447, 1321 cm^{-1} have been corresponding to OH stretching, CH and OH stretching and C-O-H bending respectively [14].

Table 4.4 FTIR spectra of polyvinyl alcohol (PVA) capped SiO_2 nanoparticles

c_1	3420 cm^{-1}	Si-OH stretching bands
c_2	1559 cm^{-1}	-OH stretching
c_3	1447 cm^{-1}	-CH and OH bending
c_4	1321 cm^{-1}	-C-O-H bending
c_5	1103 cm^{-1}	Si-O-Si stretching
c_6	960 cm^{-1}	Si-O-C stretching
c_7	798 cm^{-1}	*Si-O-Si symmetric stretching
c_8	456 cm^{-1}	Si-O-Si out of plane deformation

4.4 Conclusions:

Langmuir Blodgett monolayers of E7 nematic liquid crystal and its mixture with PVA capped SiO_2 nanoparticles were deposited on quartz substrate in Y-type mode deposition. PVA capped SiO_2 nanoparticles were characterized by Fourier Transformation Infrared Spectroscopy (FTIR). Surface pressure-area isotherm profiles were studied for each monolayer of E7 nematic liquid crystal and its mixture with PVA capped SiO_2 nanoparticles, as various phase changes were observed during constant compression of barriers. The Langmuir monolayer of E7 nematic liquid crystal shows hysteresis during multiple isotherms because of mixed amphiphilic nature of E7 nematic liquid crystal molecules while PVA capped SiO_2 nanoparticles shows no hysteresis during isotherm cycles due to elastic nature of polymer. Multiple isotherm of composite of E7 nematic liquid crystal and PVA capped SiO_2 were also observed hysteresis because larger amount of E7 nematic liquid crystal is present in these mixture. Stationary elasticity profile of monolayer has been studied as a function of mean molecular Area (MMA). Stationary elastic modulus E is an appropriate quantity for distinguishing very weak phase transitions and can be directly calculated from the slope of $\prod$-A isotherm. Normalized Area profiles decrease constantly with time ensuring about constant film compression so molecules were coming close to each other which resulted in phase change during compression isotherm. Equilibrium stabilized pressure (ESP) was attained during each deposition shows that when molecules moved

from surface to the quartz substrate then decrease in number of molecules will not result in decrease of surface pressure because barriers automatically move forward and backward to attain a constant surface pressure. Topography of monolayer of E7 nematic liquid crystal and its composite has been studied under Atomic Force Microscope.

4.5 References

1. Brugioni S. and Meucci R., European physical journal, 277, **28**, (2004).
2. Toda A., Nagano S. and Seki T., Synthetic Metals, 835, **159**, (2009).
3. Ying Y., Sheng S.C., Qiang Y.R. and Zhong M.B., Acta Physico chimica Sinica, 2217, **27**, (2011).
4. Vazquez P.G., Saavedra O.G.M., Pelzl G., Banuelos J.G. and Carreon-Castro M.P., Thin Solid Films**,** 1770**, 517,** (2009).
5. Joncheray T.J., Denoncourt K.M., Mathieu C., Meier M.A.K., Schubert U.S. and Duran R.S., Langmuir, 92, **22**, (2006).
6. Mirley C.L., Lewis M.G., Koberstein J.T., and Lee D.H.T., Langmuir, 2755, **11**, (1995).
7. Xu W., Ren F., Zhang S., Zeng G., Li T. and Wu Y., Azojomo Journal of material online, 1, **2**, (2006).
8. Butovich I.A., Arciniega J.C., and Wojtowicz J.C., Investigative Ophthalmology Visual Science, 5508, **51**, (2010).
9. Lin Y.H., Ren H., Wu Y. H., Wu S.T., Zhao Y., Fang J. and Lin H.C., Optics Express, 22, **16**, (2008).
10. Lynch M.D. and Patrick D.L., Nano Letters, 1197, **2**, (2002).
11. Singho N.D. and Johan M.R., International Journal of Electrochemical Science, 5604, **7**, (2012).
12. Zou H., Wu S. and Shen J., Chemistry Review, 3893, **108**, (2008).
13. Raju C.L., Rao J.L., Reddy B.C.V. and Brahmam K.V., Bull. Mater. Sci., 215, **30**, (2007).
14. Shao C., Kimb H.Y., Gong J., Ding B., Lee D.R. and Park S.J., Materials Letters, 1579, **57**, (2003).